

An improved performance-based plastic design method for seismic resilient fused high-rise buildings

Zhipeng Zhai^{a,b,c}, Wei Guo^{a,b,c,*}, Yaozhuang Li^a, Zhiwu Yu^{a,b,c}, Hongpeng Cao^d, Dan Bu^e

^a School of Civil Engineering, Central South University, Changsha 410075, China

^b National Engineering Laboratory for Construction Technology of High Speed Railway, Changsha 410075, China

^c Engineering Technology Research Center for Prefabricated Construction Industrialization of Hunan Province, Changsha 410075, China

^d Lanxi Municipal Engineering Management Office, Jinhua 321100, China

^e Hunan Architectural Design Institute Limited Company, Changsha 410012, China

ARTICLE INFO

Keywords:

Seismic resilient fused structure
Performance-based plastic design (PBDP)
Improved PBDP method
High-rise building
Dual system
Seismic performance

ABSTRACT

The performance-based plastic design (PBDP) method generally relies on the nonlinear response of equivalent elastic-perfectly-plastic single degree of freedom system. It usually cannot achieve the design of three performance objectives simultaneously and may not consider the high mode effect of structure, which is significant for high-rise building. In this paper, a trilinear force-displacement model indicating three prescribed performance objectives at three seismic hazard levels is adopted to improve the PBDP method. The proposed improved PBDP method is derived based on multiple degrees of freedom system, while the high-mode effect and post-yield stiffness of the structure is considered. It can be used for designing seismic resilient fused high-rise buildings. A novel dual system composed of steel energy-dissipative column (EDC) and moment resisting frame (MF) is employed for application of the proposed method. This dual system has its fuse members decoupled from the gravity-resisting system, and the performance-based design of this system is discussed as well as its application for high-rise buildings. To demonstrate the effectiveness of the proposed method, a 20-story EDC-MF structure system is designed using the improved PBDP method. A detailed numerical model of the designed EDC-MF system is then built, and nonlinear dynamic response analyses at different seismic intensities are performed to verify the actual structure performance. Results show that the designed structure can achieve the prescribed yielding mechanism and performance objectives at three seismic hazard levels, and the EDC-MF system can be effectively applied to high-rise building as a seismic resilient fused structure.

1. Introduction

In the past decade, strong earthquakes have occurred all over the world and caused great economic loss. For instance, the Wenchuan earthquake of China in 2008 caused approximately 138.33 billion USD losses; the Tohoku earthquake of Japan in 2011 led to about 30 billion USD losses; the Nepal earthquake in 2015 induced 6 billion USD losses and so on [1–6]. Therefore, resilient city and building under earthquakes have gradually become an important research focus in recent years [7,8]. The resilience is firstly defined by Sustainability Committee [9,10], which refers to the ability to suffer less damage and recover rapidly from adverse events. Specifically, buildings should be appropriately designed, so that the major functionality of buildings can be maintained and structure can be easily and rapidly repaired in a short time after severe earthquakes. However, the current seismic design codes worldwide, such as ASCE/SEI 7-10 [11], NBCC [12] and GB

50011-2010 [13], generally adopt the force-based seismic design strategy to prevent the structure from collapse, while the resilience and sustainability of the structures are still not well considered. In strong earthquakes, plastic deformation and hysteretic behavior of structures are usually designed to dissipate seismic energy which would inevitably lead to extensive response, permanent residual drift and structural damage. In general, structural components that dissipate seismic energy are also part of the gravity-resisting system in most situations [14], so the repair or replacement of seismic force-resisting components after strong earthquake is usually difficult and not viable. The damaged structural components sometimes have to be demolished even though they only suffer small or moderate damage. Hence the research and development of innovative seismic resilient fused structural system are now at the forefront of structural and earthquake engineering.

At present, the effective way for reducing structural damage and achieving earthquake resilient system is to utilize the structural fuse.

* Corresponding author at: School of Civil Engineering, Central South University, China.

E-mail address: guowei@csu.edu.cn (W. Guo).

The fuse, in the previous research, was defined as members with well-defined plastic deformation capacity, but was not necessarily replaceable [15]. Roeder and Popov [16] named the link beam of eccentric braced frame as 'ductile fuse' due to its good energy dissipation capability. Aristizabal-Ochoa [17] used the term 'structural fuse' to describe the knee member in the knee bracing steel frame system. Nowadays it's preferred that structural fuses are designed to be easily replaceable while significantly dissipate seismic energy for protecting the main structural components from damage. Several novel and efficient fuses can be adopted in multi-story buildings to reduce seismic response, such as energy dissipating shear link [18], replaceable energy dissipating moment connection [19], welded wide flange fuse [20], buckling-restrained brace [21], dual-functional replaceable stiffening angle steel component [22], steel coupling beam [23], dampers [24–27], curtain walls [29], and so forth. By rationally incorporating the fuses into the structural systems, seismic resilient system will be established. To promote seismic resilience of structure, the fuse system should be decoupled from the gravity-resisting system. All the seismic energy is supposed to be dissipated by structural fuses, and the other structural components remain elastic to bear the gravity. So the fuses can be rapidly repaired or replaced, and the building will be self-centered without residual story drift after replacing the damaged fuses. Based on this concept, some innovative seismic resilient systems have been studied. Grigorian [10] introduced the rocking core-moment frame with supplementary energy dissipating devices, and the theoretical and technical innovations were introduced to facilitate the implementation of the earthquake resilient rocking core-moment frame. Yang [14] proposed an innovative truss structure fused with buckling restrained braces and replaceable moment connections. Hamidreza [20] designed a novel resilient fused system namely Dual-Fused H-Frame, which is fused by welded wide flange fuses and buckling restrained knee braces. Shoeibi and Kafi [28] have studied the performance of linked column frame system by a new performance-based seismic design method. Li [18] has improved the steel diagrid structural system by adopting shear link fuse. Bedon [29] efficiently utilized curtain walls in multi-story buildings to markedly improve the global dynamics of structures.

To well design seismic resilient fused system, rational performance objectives at different earthquake shaking intensities should be taken into account. Performance-based seismic design (PBSD) method is the desirable approach to reach the design target. Vargas and Bruneau [15] proposed a structural fuse design procedure based on the nonlinear single degree of freedom (SDOF) which relies on results of parametric study. Medhekar and Kennedy [30] introduced the theory of displacement-based seismic design (DBSD). Yang [31] applied the DBSD to prestressed precast concrete shear walls, and Panagiotou [32] adopted the DBSD to design a 7-story building. The effectiveness of DBSD has been validated, but the target lateral displacement mode is critical but difficult to be determined in the design. Goel and Chao [33,34] introduced the performance-based plastic design (PBPD) based on the energy equilibrium concept and pre-selected yielding mechanism. Then Shoeibi [28], Qiu [35], Bai [36] and Li [18] applied the PBPD to different fused structures. As the force-deformation relationship in the PBPD is usually assumed to be bilinear, as shown in Fig. 1(a), this method cannot achieve the design of three performance objectives in one step. Recently, Yang and Dorian [14,19] proposed a novel equivalent energy design procedure (EEDP) for seismic resilient fused structures based on the response of an equivalent SDOF. The force-deformation relationship in EEDP adopts the trilinear model, which is shown as the blue line in Fig. 1(b). Therefore, this method is capable of designing three performance objectives simultaneously. In both of the PBPD and EEDP, the energy modification factor is obtained by inelastic response of equivalent SDOF, so most of the application is used only for low-rise and mid-rise building. Li [37] introduced the high-mode energy modification factor into EEDP, and applied this method to high rise fused steel diagrid frame. However, the roof drift of nonlinear

dynamic analysis didn't match well with the target roof drift. The main reasons for the discrepancies may be that the EEDP method is initially derived based on SDOF system and the high-mode energy modification factor is obtained by modifying the energy modification factor of SDOF system, which don't consider the high mode effect adequately. In addition, during the application of structural fuse, many components can increase the overall structural post-yield stiffness, which is an important aspect for the seismic damage control [38], especially when high performance materials and components are used [23,39]. Thus, the force-deformation relationship, which is shown as the red line in Fig. 1(b), is more reasonable and should be considered in practical engineering. Incorporate the post-yield stiffness into the design method will be more beneficial to control the peak displacement and residual deformation of a structure.

In this paper, a new and simple design approach considering post-yield stiffness and high-mode effect is proposed for designing seismic resilient fused structures or rehabilitating the existing buildings. This improved PBPD method is capable of simultaneously achieving three performance objectives: immediate occupancy (IO) for service level earthquakes (SLE), rapid return (RR) for design based earthquakes (DBE), and collapse prevention for maximum considered earthquakes (MCE). A novel dual system composed of steel energy-dissipative column (EDC) and moment resisting frame (MF) is employed for application of the proposed design method. Li [40] has studied the performance of EDC-MF system by a simplified lumped mass shear model, the result showed that the system can significantly mitigate the inter-story drift concentration. However, the performance-based design of this system has never been discussed, as well as its application for high-rise building. In this study, a 20-story EDC-MF structural system is designed by the proposed PBPD method. To obtain a well-designed seismic resilient system, a kind of replaceable moment connection fuse is added into the EDC-MF system. To verify the effectiveness of the improved PBPD method, finite element model (FEM) of the 20-story EDC-MF is built by OpenSees program [41], and then nonlinear time history analyses are implemented. Furthermore, seismic performance of the designed EDC-MF system is assessed.

2. Description of the traditional PBPD method

The performance-based plastic design (PBPD) method, which utilizes the pre-selected target drift and yield mechanism as key performance objectives, was developed by Goel and Chao [33,34] on the basis of energy balance concept. This method assumes that the total energy, which is needed to push a multiple degrees of freedom (MDOF) structural system monotonically up to a target drift, is equal to the energy required by an equivalent elastic-perfectly-plastic single degree of freedom (EPP-SDOF) system. The energy dissipated by the EPP-SDOF system can be estimated to be a fraction γ of the total elastic energy absorbed by an elastic single degree of freedom (E-SDOF) system. The corresponding energy balance concept is illustrated in Fig. 2. Accordingly the energy balance equation is expressed as:

$$E_e + E_p = \gamma E_i = \gamma \cdot \frac{1}{2} \frac{W}{g} \left(\frac{S_a T}{2\pi} \right)^2 \quad (1)$$

where E_i is the total input energy dissipated by the E-SDOF system; E_e and E_p are the elastic energy and plastic energy dissipated by the EPP-SDOF system, respectively; W is the structural seismic weight; T is the structural fundamental period; S_a is the first-mode spectral acceleration; g is the gravitational constant; γ is the energy modification factor, which depends on the structural ductility factor μ_s and the ductility reduction factor R_{μ} , $\gamma = (2\mu_s - 1)/(R_{\mu})^2$. The μ_s and R_{μ} can be calculated by Newmark and Hall equation [42]. The elastic energy E_e can be estimated by a SDOF system and the plastic energy E_p can be calculated according to the structural yielding mechanism and lateral force pattern [28,34,35]. By substituting the parameters into Eq. (1), the design base

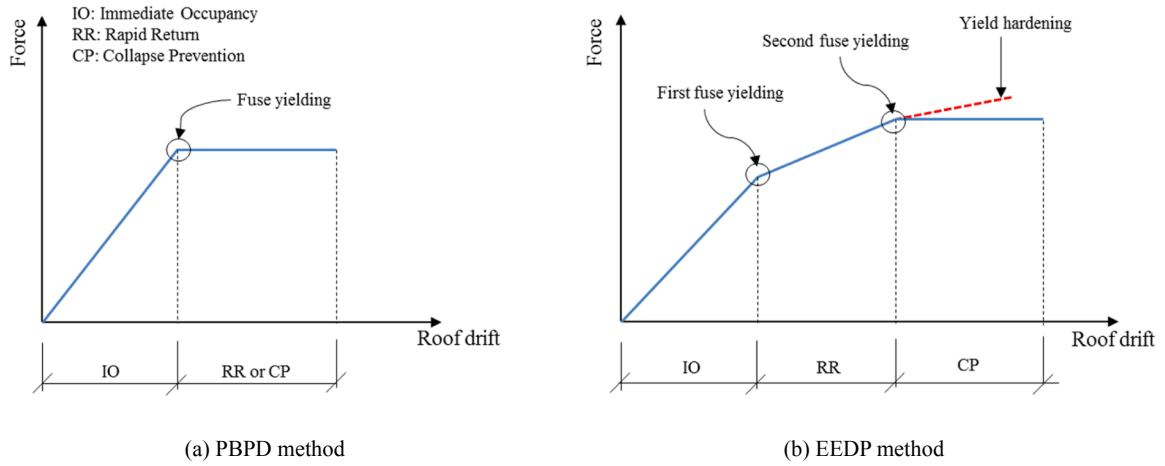


Fig. 1. Force-displacement relationship and performance objectives of fused structures.

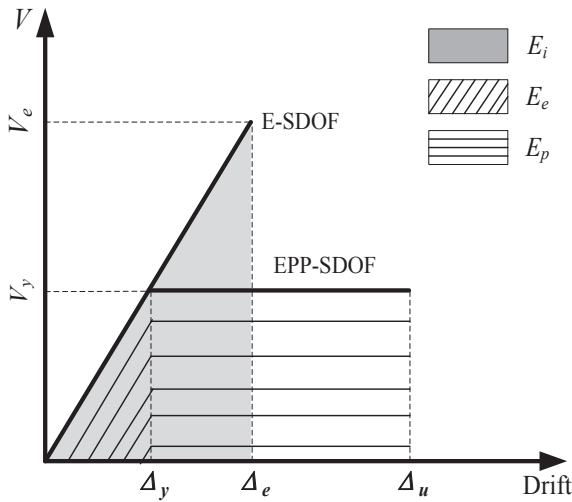


Fig. 2. Energy balance concept in PBSD method.

shear V_y can be calculated by:

$$\frac{V_y}{W} = \frac{-\xi + \sqrt{\xi^2 + 4\gamma(S_a/g)^2}}{2} \quad (2)$$

$$\xi = \frac{8\theta_p\pi^2}{T^2g} \sum_{i=1}^n C_i h_i \quad (3)$$

where C_i is the lateral force distribution factor at the i th floor; h_i is the height of the i th floor from the building base; V_y is the design base shear; θ_p is the plastic drift ratio, which is the difference between ultimate drift ratio θ_u and yielding drift ratio θ_y . Here it is assumed that all the stories have a uniform plastic drift ratio [28]. Moreover, to account for the degrading inelastic behavior or hysteretic loops with pinching, E_p should be reduced by a hysteretic energy reduction factor which is defined as the area ratio of degraded hysteretic shape to full hysteretic shape [28,34,43]. Due to stable behavior of the fuse members, the hysteretic energy reduction factor of earthquake resilient fused system in this paper is adopted as one.

3. Design procedure of the improved PBPD method

3.1. Performance objectives and design base shear

A well-designed seismic resilient fused structure is usually a dual system with the ability to achieve multiple performance objectives at

different seismic hazard levels. In the improved PBPD method of this paper, three performance design objectives are adopted. When a structure is subjected to the SLEs (e.g., with exceedance probability of 50% in 50 years), all the fuse members and structural components remain elastic, which correspond to the first performance objective IO. When structure is subjected to the DBEs (e.g., with exceedance probability of 10% in 50 years), the fuse members in primary system yield and dissipate energy by hysteretic behavior, and other structural members remain elastic, which correspond to the second performance objective RR. When structure is subjected to the MCEs (e.g., with exceedance probability of 2% in 50 years), the fuse members both in primary and secondary system enter inelastic state and the remaining structural components behaves elastically, which correspond to the third performance objective CP. During the DBE and MCE excitations, the fuses dissipate seismic energy to prevent the main structural components from damage. And after replacing the damaged fuses, the structure will return to the performance level IO. It should note that different earthquake hazard levels can be selected according to the required specific design code.

As similar to traditional PBPD method, the improved PBPD method assume that the input seismic energy can be estimated as the total elastic energy absorbed by an corresponding elastic MDOF (E-MDOF) system, and dissipated energy by the nonlinear MDOF system is estimated to be a fraction of the input seismic energy. Thus, the MDOF system has the same energy balance equation form as Eq. (1). However, the calculation of E_i , E_e , E_p and γ is different from the description in Section 2, which will be illustrated in the following section. Fig. 3 shows the force-displacement relationship and energy balance concept

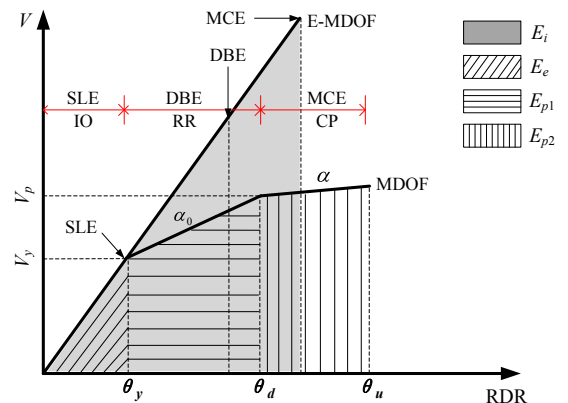


Fig. 3. Force-displacement relationship and energy balance concept in improved PBPD.

of the improved PBPD method. The horizontal axis represents the roof drift ratio (RDR), and the vertical axis represents the base shear. The force-displacement relationship of the MDOF system is simplified as trilinear model with post-yield stiffness ratio α_0 and α . As this method is directly based on a MDOF system with trilinear force-displacement model, energy modification factor used in Section 2 for traditional PBPD method is not applicable. The process of calculating design base shear is derived as below.

3.1.1. Yielding base shear for SLE excitation

Under the SLE excitation, the structure is designed to remain elastic for the performance objective IO. When a structure behaves elastically, the total elastic strain energy of an E-MDOF system, which is equal to the input seismic energy, can be approximately estimated as [35,43,44]:

$$E_i = \frac{1}{2} \frac{W}{g} \left(\frac{S_{a1} T}{2\pi} \right)^2 \quad (4)$$

where T is the fundamental period of the MDOF system; W represents the total structural seismic weight instead of first modal weight, for considering multiple vibration modes; S_{a1} is the first-mode spectral acceleration corresponding to SLE hazard level.

Akiyama [45] and Qiu [35] estimated the elastic strain energy of MDOF system by simplifying the MDOF system as an SDOF system. According to the principle of energy balance, the elastic strain energy is equal to the work of external force. Therefore, in this paper the elastic strain energy of MDOF system is approximated by:

$$E_e = \frac{1}{2} \sum_{i=1}^n (C_i V_y)(h_i \theta_y) = \frac{1}{2} \theta_y V_y \sum_{i=1}^n C_i h_i \quad (5)$$

where V_y is the yielding base shear of MDOF system; θ_y is the yielding RDR, which can be arbitrarily selected by designers for the performance objective IO; the lateral force distribution factor C_i can be determined by the selected lateral force pattern.

Because the structure remains elastic during SLE excitation, the corresponding plastic strain energy E_p and energy modification factor γ equal to zero and one, respectively. By substituting Eqs. (4) and (5) into Eq. (1), the following formula can be given:

$$V_y = \frac{W}{g} \left(\frac{S_{a1} T}{2\pi} \right)^2 / \left(\theta_y \sum_{i=1}^n C_i h_i \right) \quad (6)$$

The yielding base shear can be easily determined by Eq. (6). However, the fundamental period of the structure, T , is generally unknown at the beginning of design. It needs to estimate the T at the initial design, and iteration may be necessary during the design process. If the T of a designed structure is far from the initial assumption, it must be adjusted until the value of T converges to the final design value. In order to reduce the iteration, the fundamental period is needed to be rationally estimated. An effective way, based on the elastic displacement spectrum and displacement-based seismic design [30], is utilized here for estimating the fundamental period. If the uniform mass distribution along the structural height is adopted, the spectral displacement, S_d , of an equivalent SDOF system can be expressed as:

$$S_d = u_{eff} = \frac{\sum_{i=1}^n m_i u_i^2}{\sum_{i=1}^n m_i u_i} = \frac{\sum_{i=1}^n h_i^2}{\sum_{i=1}^n h_i} \theta_y \quad (7)$$

where u_{eff} is the drift of equivalent SDOF system; u_i is the drift at i th floor of MDOF system, which is approximated by $h_i \theta_y$; here; m_i is the i th floor mass. Moreover, an elastic design displacement spectrum corresponding to the SLE excitation can be obtained according to the design acceleration spectrum in seismic code. After determining S_d by Eq. (7), the fundamental period can be estimated by the design displacement spectrum.

3.1.2. Plastic base shear for DBE excitation

During the DBE excitation, fuse members of primary system enter inelastic state, while the other structural members are elastic. From the SLE level to DBE level, the plastic energy needed for pushing structure to the target performance state produces, and is remarked as E_{p1} . During this process, an energy modification factor γ_a is introduced into the energy balance equation:

$$E_e + E_{p1} = \gamma_a E_i \quad (8)$$

According to the description in the previous section, the total input energy and the elastic strain energy are estimated by Eqs. (9) and (10), respectively. Based on the balance principle of internal and external virtual work, the plastic energy dissipated by the structure can be computed by Eq. (11). Among these equations, S_{a2} is the first-mode spectral acceleration corresponding to DBE excitation; θ_{p1} is the plastic drift ratio at the DBE excitation, which is calculated by $\theta_{p1} = \theta_d - \theta_y$, and θ_d is determined by designers to target the performance objective RR; V_p is the plastic base shear corresponding to DBE level. As the same with the PBPD method, all the stories are assumed to have a uniform plastic drift ratio.

$$E_i = \frac{1}{2} \frac{W}{g} \left(\frac{S_{a2} T}{2\pi} \right)^2 \quad (9)$$

$$E_e = \frac{1}{2} \frac{W}{g} \left(\frac{S_{a1} T}{2\pi} \right)^2 \quad (10)$$

$$E_{p1} = \frac{1}{2} \sum_{i=1}^n (C_i V_y + C_i V_p)(h_i \theta_{p1}) = \frac{1}{2} \theta_{p1} (V_y + V_p) \sum_{i=1}^n C_i h_i \quad (11)$$

By substituting Eqs. (9)–(11) into (8), the plastic base shear can be solved as Eq. (12). The energy modification factor γ_a will be described in detail in the following section.

$$V_p = \frac{W}{g} \left(\frac{T}{2\pi} \right)^2 (\gamma_a S_{a2}^2 - S_{a1}^2) / \left(\theta_{p1} \sum_{i=1}^n C_i h_i \right) - V_y \quad (12)$$

3.1.3. Ultimate RDR for MCE excitation

During the MCE excitation, the fuse members both in primary and secondary system are designed to dissipate energy via plastic deformation, and the main structural members remain elastic. The performance objective CP is achieved in this hazard level by designing structural fuses to maintain their yielding strength until the structure reaches the ultimate RDR θ_u [19]. The incremental plastic energy produced from the DBE to MCE excitation is remarked as E_{p2} . And an energy modification factor γ_b is introduced into the energy balance equation:

$$E_e + E_{p1} + E_{p2} = \gamma_b E_i \quad (13)$$

The energy modification factor γ_b will be described in detail in the following section. According to the description in the previous section, the total input energy and the elastic strain energy are estimated by Eqs. (14) and (10), respectively. Based on the balance principle of internal and external virtual work, the incremental plastic energy can be computed by Eq. (15). In these equations, S_{a3} is the first-mode spectral acceleration corresponding to MCE hazard level; θ_{p2} is the plastic drift ratio from the DBE to MCE hazard level, which is calculated by equation: $\theta_{p2} = \theta_u - \theta_d$.

$$E_i = \frac{1}{2} \frac{W}{g} \left(\frac{S_{a3} T}{2\pi} \right)^2 \quad (14)$$

$$E_{p2} = V_p \theta_{p2} \sum_{i=1}^n C_i H_i + \frac{1}{2} \alpha \frac{V_y}{\theta_y} \theta_{p2}^2 \sum_{i=1}^n C_i H_i \quad (15)$$

By substituting Eqs. (10)–(11), and (14)–(15) into (13), the ultimate RDR can be given as:

$$\theta_u = \theta_d + \theta_{p2} = \theta_d + \frac{-V_p + \sqrt{V_p^2 + \lambda\alpha \left(V_y / \theta_y \sum_{i=1}^n C_i H_i \right)}}{\alpha(V_y/\theta_y)} \quad (\alpha \neq 0) \quad (16a)$$

$$\text{or } \theta_u = \theta_d + \lambda / \left(V_p \sum_{i=1}^n C_i H_i \right) \quad (\alpha = 0) \quad (16b)$$

$$\lambda = \frac{W}{g} \left(\frac{T}{2\pi} \right)^2 (\gamma_b S_{a3}^2 - \gamma_a S_{a2}^2)$$

3.2. Lateral force pattern and P-Delta effect

3.2.1. Lateral force pattern

Several lateral force patterns presented in current seismic design codes [11,13,46,47] are available for structural analysis and design, but these patterns are generally based on the elastic response of MDOF systems [45]. In this paper, a modified lateral force pattern, which is derived from extensive nonlinear dynamic analyses by Chao et al. [48], is adopted and expressed as follows:

$$F_i = C_i V \quad (17)$$

$$C_i = (\beta_i - \beta_{i+1}) \left(\frac{w_n h_n}{\sum_{j=1}^n w_j h_j} \right)^{qT^{-0.2}} \quad (18)$$

$$\beta_i = \frac{V_i}{V_n} = \left(\frac{\sum_{j=i}^n w_j h_j}{w_n h_n} \right)^{qT^{-0.2}} \quad (19)$$

where F_i is the lateral force at i th floor; V is the design base shear; C_i is the lateral force distribution factor and T is the fundamental period as mentioned above; β_i is the shear distribution factor at the i th floor; V_i and V_n are the story shear force at the i th floor and roof, respectively; W_j and W_n are the structural seismic weight at i th floor and roof, respectively; h_j and h_n are the height of i th floor and roof from the base, respectively. The value of parameter q that affects the distribution of lateral force along the structural height can be modified for different structural systems. Here, the value 0.75 suggested by previous study [48] is adopted for q to consider the structural high mode effect.

3.2.2. P-Delta effect

The P-Delta effect, which may cause structural instability, is critical for design of high-rise building. In current seismic design codes, such as ASCE 7-10 [11], it is considered through the stability coefficient and additional base shear. Because the design elastic displacement is used in these codes, and inelastic displacement would lead to economic inefficiency design, Shoeibi [28] defined a modified stability coefficient as:

$$SC_i = \frac{\Delta_{y,i} \sum_{j=i}^n P_j}{V_{y,i} h_i} = \frac{\sum_{j=i}^n P_j}{V_{y,i}} \theta_y \quad (20)$$

where SC_i is the stability coefficient; P_j is the gravity load at j th floor; $\Delta_{y,i}$ is the story displacement of i th floor and $V_{y,i}$ is the story shear of i th floor, which are resulted from yielding base shear. When SC_i is lower than 10%, the P-Delta effect can be ignored. Otherwise, the additional base shear, computing by Eq. (21), should be added to the base shear of the building.

$$V_a = \theta_y \sum_{i=1}^n P_i \quad (21)$$

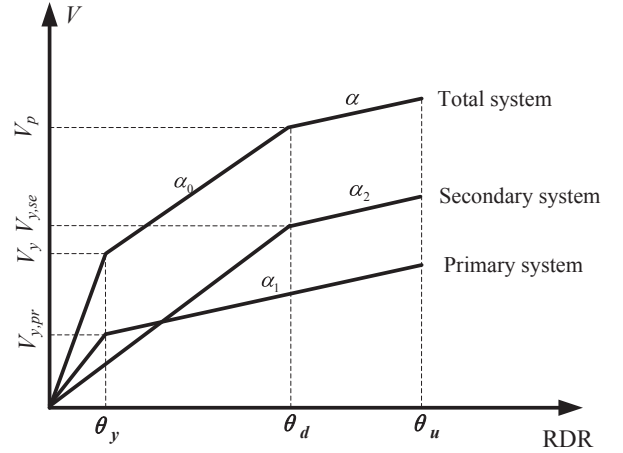


Fig. 4. Distribution of design base shear between primary and secondary system.

3.3. Distribution of design base shear and the design procedure

3.3.1. Distribution of design base shear to the primary and secondary system

Fuse members in the primary and secondary system are designed to dissipate seismic energy at the DBE and MCE hazard level, respectively. And structural fuses maintain their yielding strength even while the structure reaches the ultimate response RDR. Hence, the force-displacement relationships of the total, primary and secondary system can be described as Fig. 4. The sum of primary and secondary system's base shear equals to that of the total system. Considering this force equilibrium condition, the following equations can be obtained:

$$V_{y,pr} = \frac{V_p - \mu_d V_y}{(\alpha_1 - 1)(\mu_d - 1)} \quad (22)$$

$$V_{y,se} = \frac{[1 + \alpha_1(\mu_d - 1)]V_y - V_p}{(\alpha_1 - 1)(\mu_d - 1)} \mu_d \quad (23)$$

where $V_{y,pr}$ and $V_{y,se}$ are the yielding strength of the primary and secondary system, respectively; the ductility factor μ_d is defined as the ratio of θ_d to θ_y ; α_1 is post-yield stiffness ratio of the primary system. The relationship of secondary system's post-yield stiffness ratio α_2 , α_1 and α can be expressed as:

$$\alpha_1 \frac{V_{y,pr}}{\theta_y} + \alpha_2 \frac{V_{y,se}}{\theta_d} = \alpha \frac{V_y}{\theta_y} \quad (24)$$

when the same materials and components are used for primary and secondary fuse system, that is α_1 equals α_2 , it can be obtained that $\alpha_1 = \alpha_2 = \alpha$.

3.3.2. Design procedure

After distributing the design base shear to primary and secondary system, plastic design for the fuse members and capacity design for the non-yielding members can be implemented for achieving a seismic resilient structure. The design flowchart of the proposed PBPD method is plotted in Fig. 5, and the design steps are outlined as follows.

- (1) Specify the structural parameters, including the story number n , the story height h_i and weight w_i . Select the type of structural fuse and determine the post-yield stiffness ratio α_1 and α_2 . If the structural fuse of each system utilize the same material, it is that $\alpha_1 = \alpha_2$.
- (2) Select the seismic hazard levels and target RDR θ_y for performance level IO. According to the design response spectra, estimate the structural fundamental period T by Eq. (7).
- (3) Calculate parameters of lateral force pattern C_i and β_i which

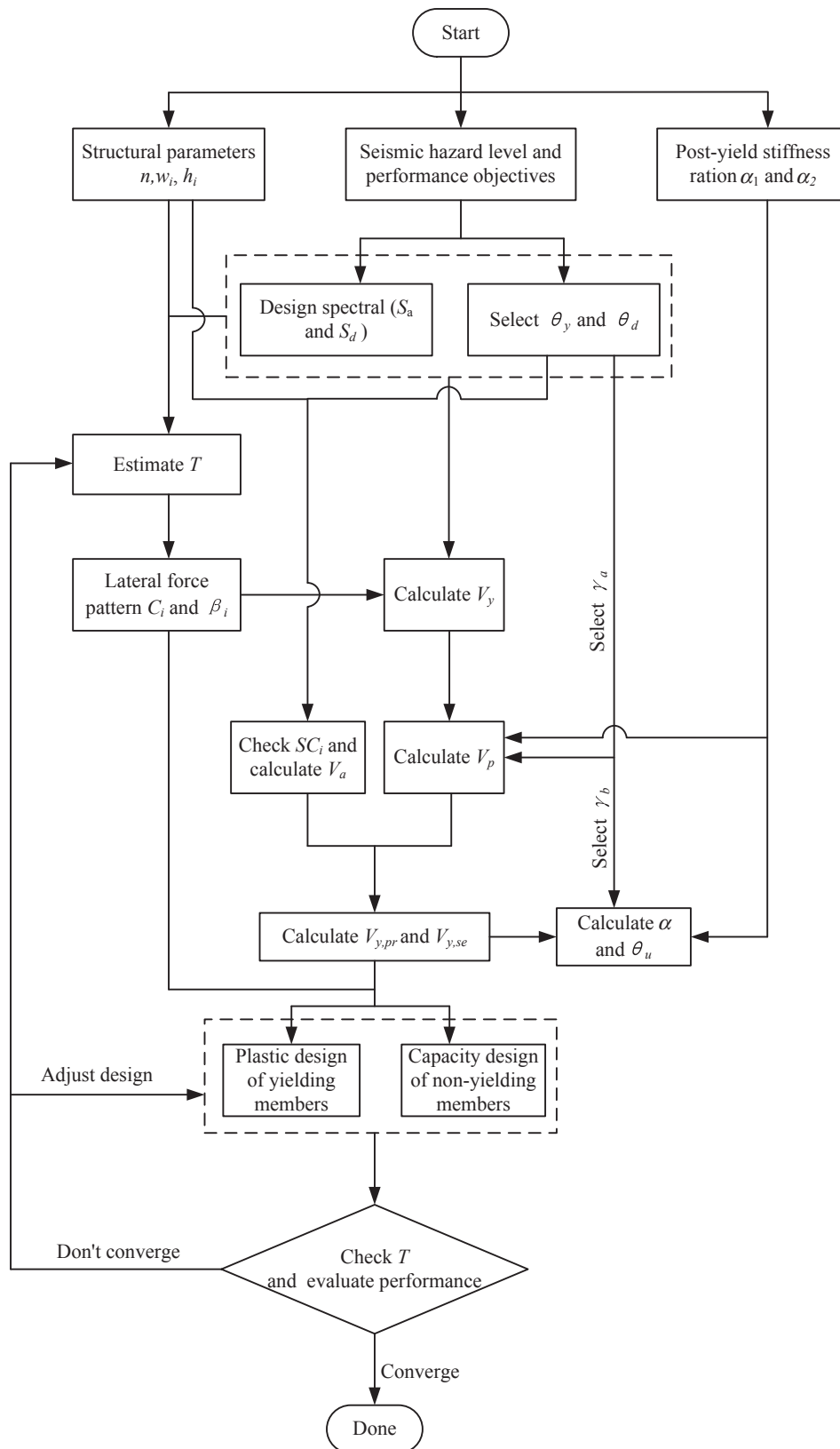


Fig. 5. Design flowchart of the proposed PBPD method.

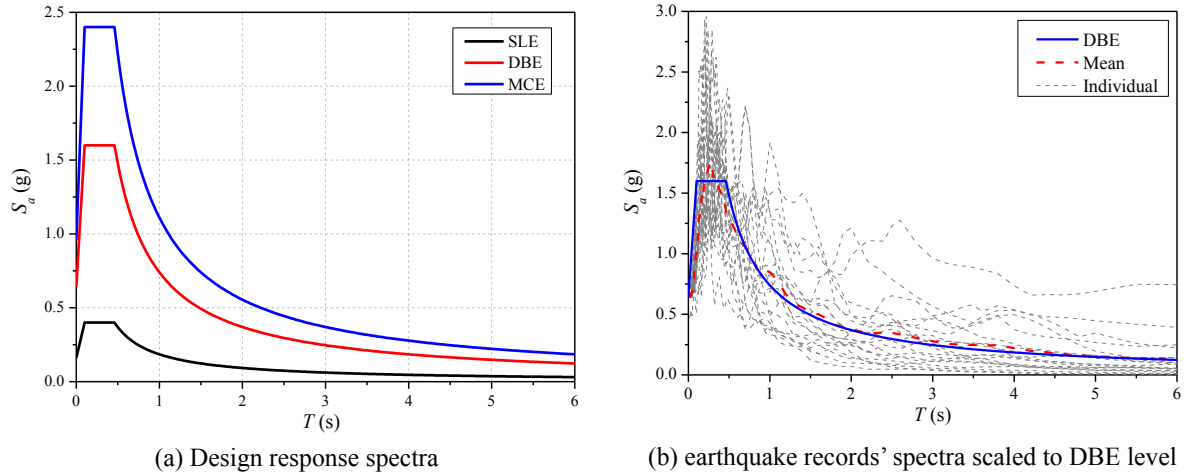


Fig. 6. Response spectra of ASCE 7-10 and earthquake records.

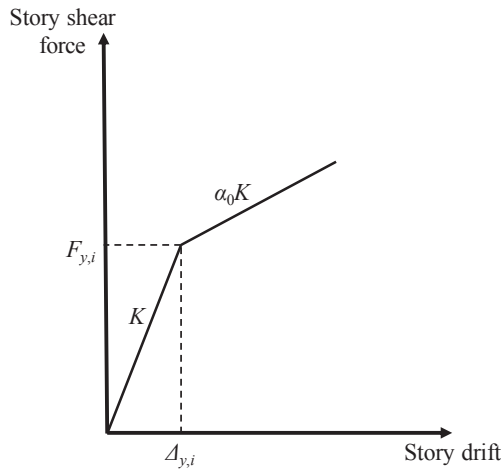


Fig. 7. The shear force-displacement relationship at the i th story for determining γ_a .

consider the high mode effect. Then calculate the yielding base shear V_y by Eq. (6).

- (4) Select target RDR θ_p for performance level RR, and calculate plastic RDR and ductility factor by $\theta_{p1} = \theta_p - \theta_y$ and $\mu_d = \theta_p / \theta_y$. Then, determine energy modification factor γ_a described in following section, and calculate the plastic base shear V_p by Eq. (12).
- (5) Check the stability coefficient using Eq. (20), and calculate additional base shear V_a for considering P-Delta effect by Eq. (21) if necessary.
- (6) Distribute the design base shear to primary and secondary system, and calculate the yielding strength, $V_{y,pr}$ and $V_{y,se}$, by Eqs. (22) and (23).
- (7) Calculate post-yield stiffness ratio α through Eq. (24), if $\alpha_1 = \alpha_2$, it can be obtained that $\alpha_1 = \alpha_2 = \alpha$. Then, determine energy modification factor γ_b described in following section and calculate the ultimate RDR θ_u to target performance level of CP by Eq. (16).
- (8) Determine lateral force F_i at each floor of primary and secondary system through Eq. (17). And design the yielding members (fuses in each system) using plastic design process. During the member design, general provisions in design codes, such as GB 50011-2010 [13] and AISC 341-10 [49], can be taken into account. Because the design code is utilized to design or adjust the member's section and has no effect on the pre-selected yielding mechanism, different design codes can be used without considering the possible differences.

- (9) Design the non-yielding members according to the capacity design principle, to ensure that these members remain elastic under the probable forces created by the yielding members. During the design, the factor $1.25R_y$ and $1.1R_y$ can be considered for non-yielding members of primary and secondary system, respectively, where R_y is the ratio of expected yield stress to the specified yield stress [28].
- (10) Check the fundamental period T . If T is far from the initial assumption, return to step 3.
- (11) If T converges to the final design value, the seismic performance of the final designed structure should be evaluated via nonlinear dynamic analysis.

3.4. Energy modification factors

3.4.1. Ground motions

The energy modification factors in the PBBP and EEDP methods are derived by nonlinear time history analysis of SDOF system. To design a high-rise fused steel diagrid frame utilizing EEDP method, Li [37] has implemented nonlinear time history analysis of MDOF system to adjust the energy modification factors. Similarly, the two energy modification factors of the proposed method in this paper, γ_a and γ_b , which are required for achieving three performance objectives at three seismic hazard levels, will be derived by a series of nonlinear time history analyses. A suite of 20 ground motions, are selected from the PEER ground motion database [50], as listed in Table A1. These ground motions are selected based on the site class C soil specified in ASCE 7-10 [11]. The design spectral parameters, SM_s and SM_1 , for MCE (2% probability of exceedance in 50 years) are 2.4 and 1.1, respectively. The design spectral parameters, SD_s and SD_1 , for DBE (2% probability of exceedance in 50 years) are 1.6 and 0.74, respectively [11]. The design spectrum of SLE level adopts 25% of the DBE level spectrum, representing 87% probability of exceedance in 50 years [14,37,51]. Fig. 6 shows the design response spectra specified in ASCE 7-10 [11], and spectra of the selected earthquake records scaled to DBE level.

3.4.2. Energy modification factor γ_a

The proposed method is directly based on MDOF system. Hence, the energy modification factors are determined here by nonlinear dynamic analysis of MDOF system, which considers the structural high mode effect. γ_a is the energy modification factor for performance level RR with the target RDR θ_d . For a selected θ_d , relationship of post-yield stiffness ratio α_0 , μ_d and γ_a can be expressed as:

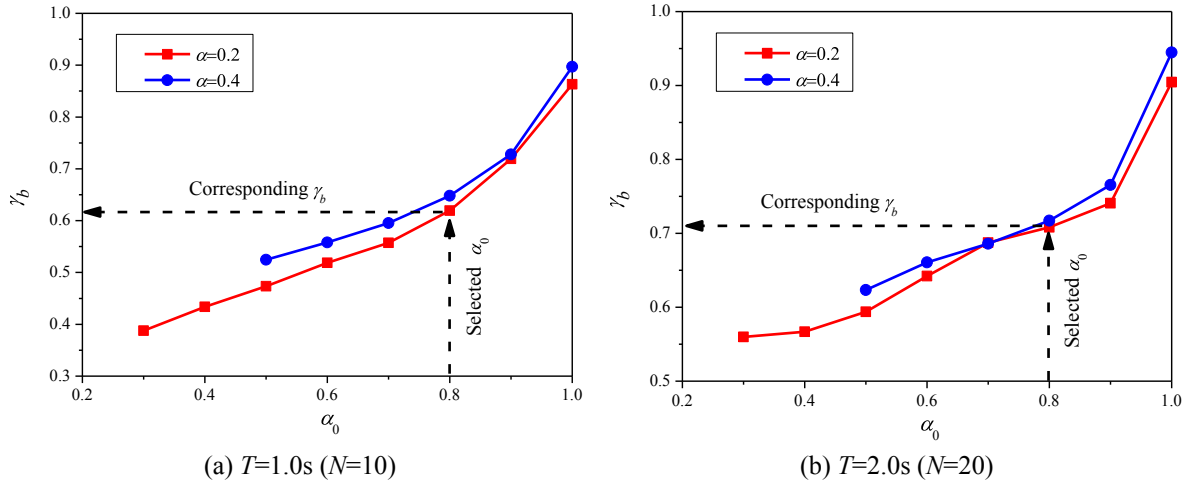


Fig. 10. Determination of energy modification factor γ_b .

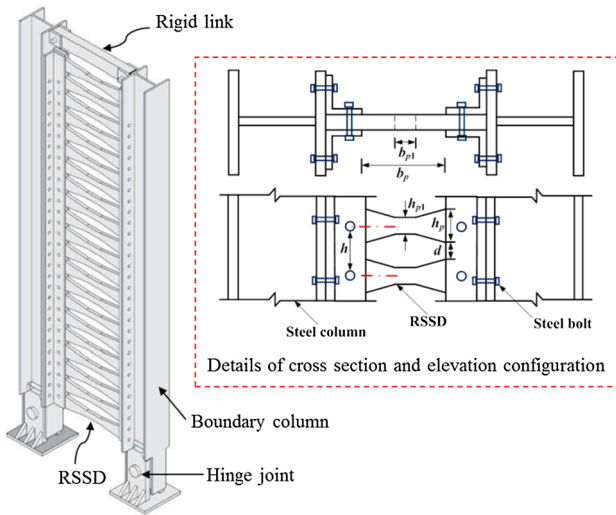


Fig. 11. Configuration details of EDCs.

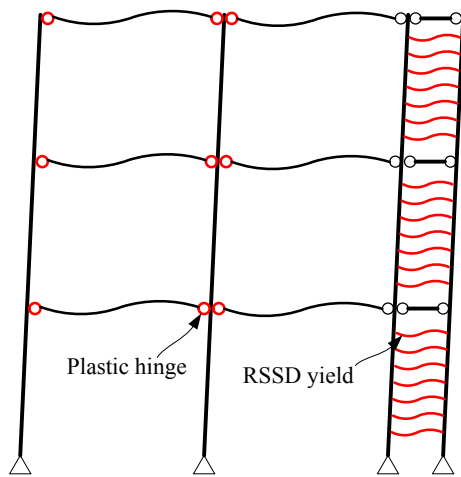


Fig. 12. Failure mode of EDC-MF system.

(4) Test different T and n , and obtain different relation curve of α_0 , μ_d and γ_a .

During the analysis, 2.5% Rayleigh damping is adopted. The flow-chart for determining γ_a is provided in Fig. A1, and calculating results with $T = 1.0$ s (storey number $n = 10$) and $T = 2.0$ s ($n = 20$) are described in Fig. 8.

3.4.3. Energy modification factor γ_b

γ_b is the energy modification factor for performance objective CP under MCE level excitation. Based on the previous section, the steps for determining γ_b are outlined as follows.

- (1) Select parameter α which is smaller than α_0 . Then, force-displacement relationship at the i th story can be plotted in Fig. 9, and trilinear lumped mass story model can be established. Perform non-linear time history analysis for this analytical model, and then determine RDR $\theta_{r,MCE}$.
- (2) Calculate γ_b by Eq. (16) according to $\theta_{r,SLE}$, $\theta_{r,DBE}$, $\theta_{r,MCE}$ and base shear of elastic model and bilinear analytical model.
- (3) Try different α_0 and obtain the relation curve of α_0 and γ_b .
- (4) Test different T and α , and obtain different relation curve of α_0 and γ_b .

The flowchart for determining γ_b is described in Fig. A2, and calculating results when $\alpha = 0.2$ and $\alpha = 0.4$ are shown in Fig. 10.

4. Application of the improved PBD method

4.1. The EDC-MF dual system

A novel structural system, EDC-MF dual system, introduced by Li [40] is adopted to illustrate the application of proposed design method. The EDC-MF system consists of steel energy-dissipative column (EDC) and moment resisting frame (MF). The EDC consists of two steel boundary columns connected by a series of replaceable steel strip dampers (RSSD). And at each story level, a rigid link is used to coordinate deformation of the two columns. Fig. 11 shows the configuration details of EDCs [55,56]. Experimental studies of EDCs were conducted by Li [55], and the theoretical formulas for determining the elastic stiffness, yielding and ultimate capacity of the EDCs are derived [56]. Moreover, performance of EDC-MF system has been studied by a simplified lumped mass shear model [40], the result showed that the system can significantly mitigate the inter-story drift concentration. However, the performance-based design of this system has never been

Then, conduct nonlinear time history analysis of this analytical model, and determine RDR $\theta_{r,DBE}$.

- (3) Calculate μ_d by $\mu_d = \theta_{r,DBE}/\theta_{r,SLE}$, and γ_a by Eq. (25). Try different α_0 and obtain the relation curve of α_0 , μ_d and γ_a .

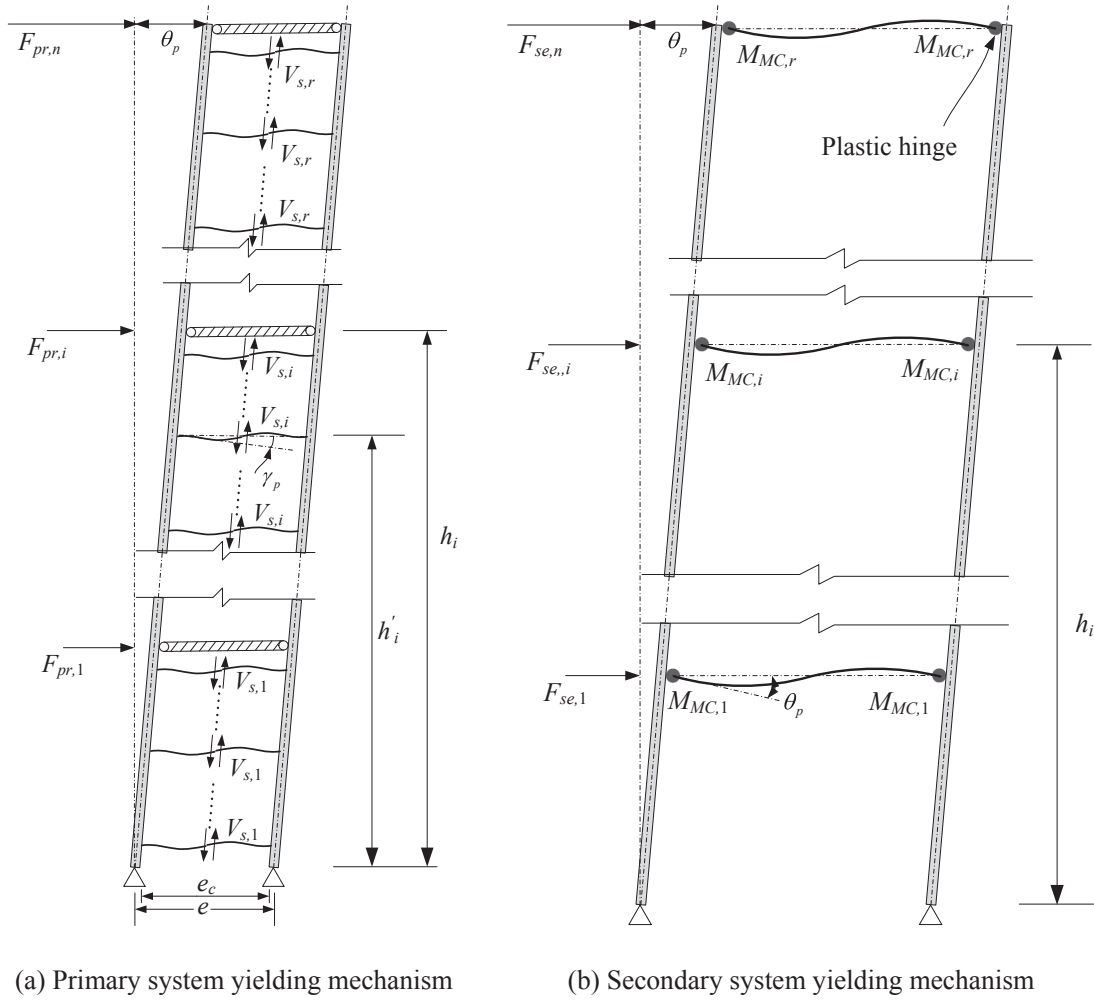


Fig. 13. Yielding mechanism of EDC-MF system.

discussed, as well as its application for high-rise buildings.

During the test of EDC in literature [55], the boundary columns still remained elastic at the end of test. And desirable failure model of the EDC-MF system is dominated by ductile rupture of RSSDs and plastic hinge development in ductile beams, as shown in Fig. 12. Therefore, EDC-MF has great potential to be designed as a seismic resilient structure. The fuses, RSSD, are replaceable and decoupled from the gravity system. It needs to introduce a type of replaceable moment connection into the EDC-MF system. The bolted moment connection (MC) proposed by Pryor and Murray [57], as shown in Fig. A3 [19], is utilized here. This connection consists of steel angel and yielding plates. The yielding plates are designed to absorb seismic energy by tension and compression deformation as a result of joint rotation. It is decoupled from the gravity-resisting system due to steel angle is designed to support gravity loads when the plates are damaged and need to be replaced. With these two types of fuse, the EDC-MF system can be developed as a well-designed seismic resilient structural system.

4.2. Structural member design

4.2.1. Plastic design of yielding members

Here the improved PBPD method in this paper is adopted for the design of EDC-MF system. The fuses in primary system are designed to yield firstly. Its yielding mechanism is plotted in Fig. 13(a). The shear forces of RSSDs at the same floor are assumed to be equal, remarked as $V_{s,i}$, which is computed as $\beta_i V_{s,r}$. $V_{s,r}$ is the shear force of RSSDs in the top floor. Because the RSSDs evenly distribute in each floor, the height

from middle of the story to the base h'_i is used to calculate β_i here. According to kinematic energy equilibrium method, $V_{s,r}$ can be determined as follows:

$$\begin{aligned}
 W_{ext,pr} &= \frac{1}{2} \left(\alpha_1 \frac{\theta_p}{\theta_y} + 2 \right) \sum_{i=1}^n F_{pr,i} h_i \theta_p \\
 W_{int,pr} &= \sum_{i=1}^n n_s V_{s,i} (e_c \gamma_p) \\
 \gamma_p &= e \theta_p / e_c \\
 V_{s,i} &= \beta_i V_{s,r} \\
 V_{s,r} &= \frac{\left(\alpha_1 \frac{\theta_p}{\theta_y} + 2 \right) \sum_{i=1}^n F_{pr,i} h_i}{2 n_s e \sum_{i=1}^n \beta_i} \quad (28)
 \end{aligned}$$

where $W_{ext,pr}$ and $W_{int,pr}$ are the external work internal work of primary system, respectively; θ_p is the plastic drift ratio and should be computed by $\theta_p = \theta_u - \theta_y$ here; $F_{pr,i}$ is the lateral force distribution of primary system; γ_p is the shear rotation of RSSD; e and e_c are the bay length and clear bay length of EDC, respectively; n_s is the number of RSSD in each story. Based on the theoretical formulas of yielding capacity of RSSDs [56], the primary fuses, RSSDs, can be designed by Eq. (29), where Q_y is the yielding capacity of RSSD, and meaning of other items are shown in Fig. 11. The b_{p1}/b_p and h_{p1}/h_p are respectively suggested to be 0.25 and 0.5 in previous studies [55,56].

$$V_{s,i} = Q_y = \frac{4R_y f_y t_p h_p^2 (h_{p1}/h_p - b_{p1}/b_p)(1 - h_{p1}/h_p)}{3(1 - b_{p1}/b_p)^2 b_p} \quad (29)$$

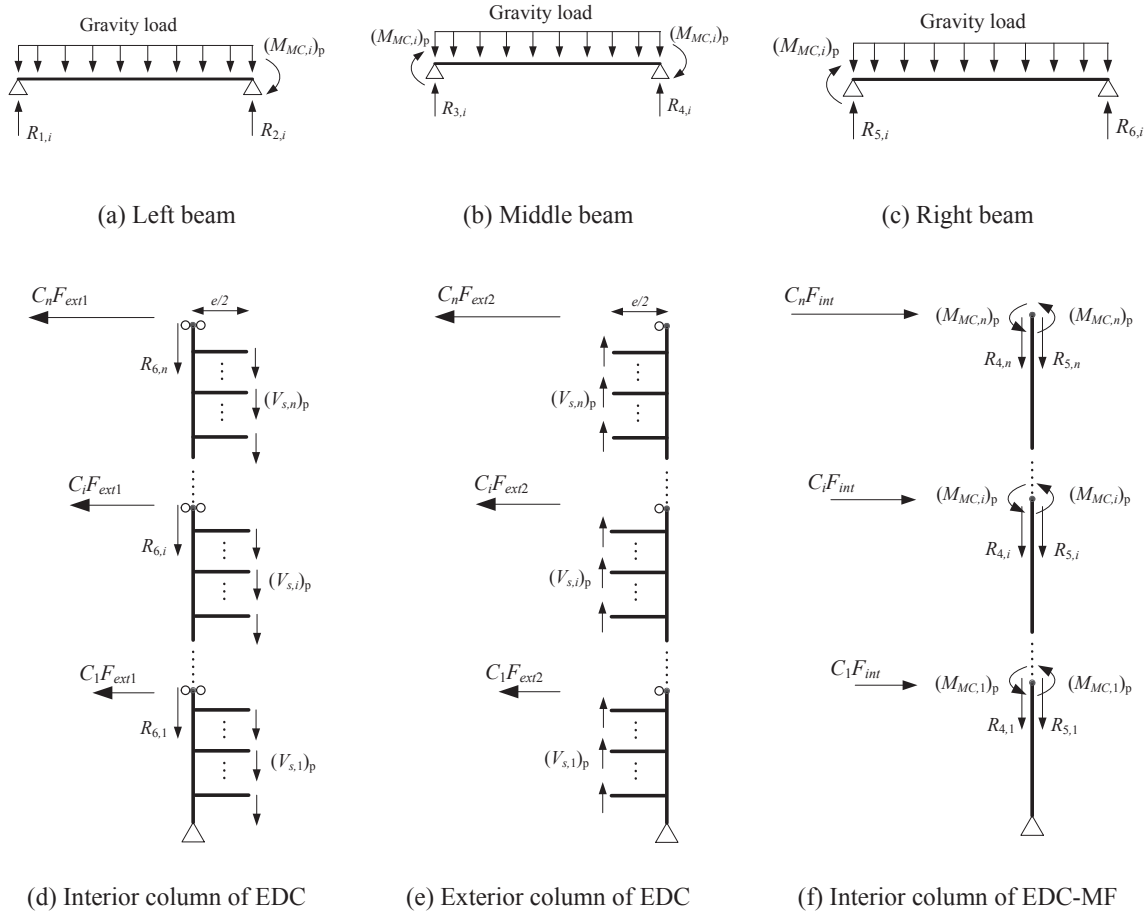


Fig. 14. Free body diagram for the capacity design.

Fig. 13(b) shows the yielding mechanism of secondary system. Plastic hinges form at end of the beams due to the MCs yield. The design moment of MCs at top floor is $M_{MC,r}$ and then moment of MCs at i th floor $M_{MC,i}$ is calculated as $\beta_i M_{MC,r}$. Using kinematic energy equilibrium method, $M_{MC,r}$ can be determined as follows:

$$\begin{aligned}
 W_{ext,se} &= \frac{1}{2} \left(\alpha_2 \frac{\theta_p}{\theta_d} + 2 \right) \sum_{i=1}^n F_{se,i} h_i \theta_p \\
 W_{int,pr} &= \sum_{i=1}^n n_c M_{MC,i} \theta_p \\
 M_{MC,i} &= \beta_i M_{MC,r} \\
 M_{MC,r} &= \frac{\left(\alpha_2 \frac{\theta_p}{\theta_d} + 2 \right) \sum_{i=1}^n F_{se,i} h_i}{2 n_c \sum_{i=1}^n \beta_i}
 \end{aligned} \tag{30}$$

where $W_{ext,se}$ and $W_{int,pr}$ are the external work internal work of secondary system, respectively; the plastic drift ratio θ_p should be calculated by $\theta_p = \theta_u - \theta_d$ here; $F_{se,i}$ is the lateral force distribution of secondary system; n_c is the number of MC in each story. Then, the area of yielding plate in MC at each floor, A_i , can be designed by Eq. (31), where f_y is the specified yielding strength of the steel plate, d_i is the depth of the beam at i th floor, and R_y adopts 1.1 [19].

$$A_i = \frac{M_{MC,i}}{R_y f_y d_i} \tag{31}$$

4.2.2. Capacity design of non-yielding members

After the yielding members have been designed, the non-yielding members (beams and columns) need to be capacity designed to remain elastic under the maximum probable forces created by RSSDs and MCs.

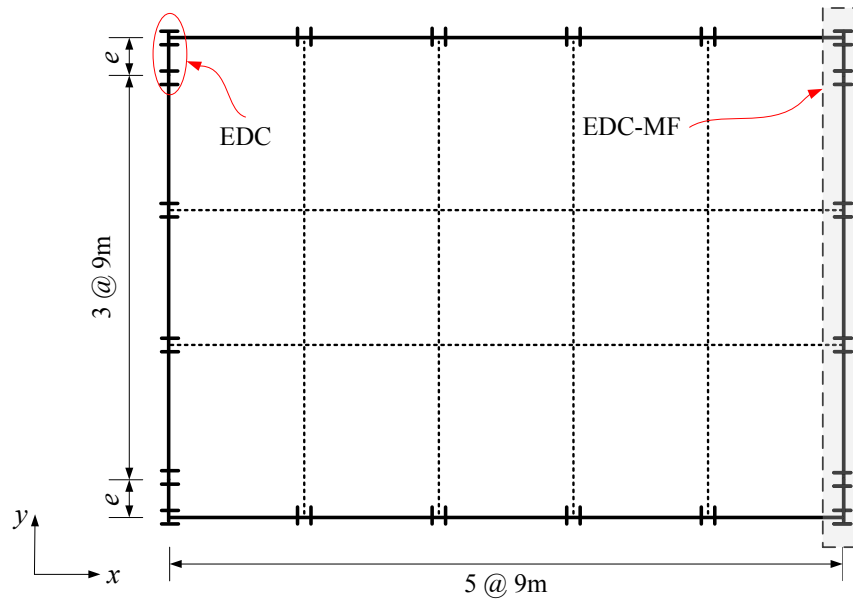
Fig. 14 shows the free body diagram for the design of beams and columns, which adopts the same structural arrangement as the design example in Section 4.3. Although the arrangement of EDCs may be different in other structures, the method of establishing

free body diagram is identical. The subscript ‘p’ means the maximum probable forces. The unbalanced lateral forces, $C_i F$, in Fig. 14(d)–(f) can be calculated by taking moment about the column base, where the moment resulted by all the forces should be zero. It should be noted that all loads including gravity load should be considered during the process of capacity design.

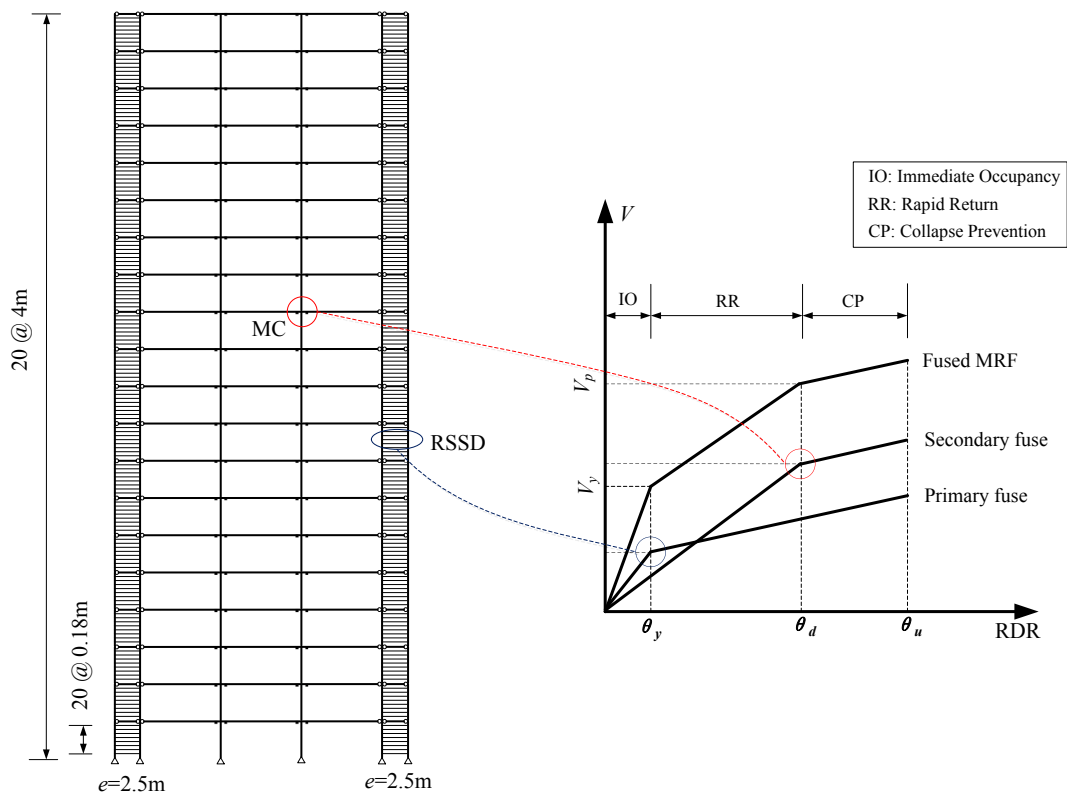
4.3. Design example of EDC-MF system

The prototype building, a 20-story EDC-MF with 5×3 bays, is designed to demonstrate the applicability of the proposed design method in this paper. The bay width of the moment frame and EDC are 9 m and 2.5 m, respectively. The story height is 4 m. The parameters, h and h_p , for RSSD are 0.18 m and 0.15 m, respectively. There are 42 RSSDs (two EDCs) and 4 MCs in each floor. According to the experimental studies [19,55,57], the parameters, α_1 , α_2 and α , adopt 0.2. All the columns are pin connected to the base. Fig. 15 shows plan layout and elevation view of the prototype structure, as well as the performance objectives. The building is symmetric in both x and y direction, and only one bay in the y direction is studied in this paper. The seismic tributary mass for the one-bay EDC-MF is 40702.5 kN, which equals to 1/6 of the total structural mass. The structure is assumed to locate at the site class C soil specified in ASCE 7-10 [11], and the design spectral parameters have been described in Section 3.4.1.

The steel material with yielding stress of 235 MPa is used for the primary fuses (RSSDs). Other members, including secondary fuses



(a) Plan view



(b) Elevation view and performance objectives

Fig. 15. Plan and elevation view of prototype 20-story EDC-MF system.

Table 1
Design parameters of proposed PBPD method.

Parameters	Value	Remark	Parameters	Value	Remark	Parameters	Value	Remark
W/kN	40702.5	Given	S_{a2}/g	0.37	ASCE 7-10	V_y	0.084 W	Eq. (6)
$\alpha_1, \alpha_2, \alpha$	0.2	Given	S_{a3}/g	0.555	ASCE 7-10	V_p	0.166 W	Eq. (12)
RDR θ_y	0.17%	User-defined	μ_t	3.4	θ_d/θ_y	RDR θ_u	1.04%	Eq. (16)
RDR θ_d	0.58%	User-defined	α_0	0.4	Fig. 8(b)	$V_{y,pr}$	0.062 W	Eq. (22)
T/s	2.0	Eq. (7)	γ_a	0.51	Fig. 8(b)	$V_{y,se}$	0.074 W	Eq. (23)
S_{a1}/g	0.0925	ASCE 7-10	γ_b	0.57	Fig. 10(b)			

Table 2
The member sections designed by proposed PBPD method.

Story	Column in EDC	Interior column	Beam	$t_p \times h_p \times b_p$ of RSSD (m)	Yielding plate area of MC (m ²)
1	W36 × 800	W36 × 361	W24 × 279	0.085 × 0.15 × 1.2	0.013
2	W36 × 800	W36 × 361	W24 × 279	0.085 × 0.15 × 1.2	0.013
3	W14 × 730	W14 × 730	W24 × 279	0.085 × 0.15 × 1.2	0.013
4	W14 × 665	W14 × 730	W24 × 229	0.085 × 0.15 × 1.2	0.013
5	W14 × 665	W14 × 730	W24 × 229	0.100 × 0.15 × 1.5	0.013
6	W14 × 550	W14 × 730	W24 × 229	0.100 × 0.15 × 1.5	0.012
7	W14 × 500	W14 × 730	W24 × 229	0.100 × 0.15 × 1.5	0.012
8	W14 × 455	W14 × 730	W24 × 207	0.100 × 0.15 × 1.5	0.012
9	W14 × 426	W14 × 665	W24 × 207	0.095 × 0.15 × 1.5	0.012
10	W14 × 370	W14 × 665	W24 × 207	0.090 × 0.15 × 1.5	0.011
11	W14 × 342	W14 × 665	W24 × 192	0.090 × 0.15 × 1.5	0.011
12	W14 × 283	W14 × 605	W21 × 201	0.085 × 0.15 × 1.5	0.011
13	W14 × 233	W14 × 605	W21 × 201	0.080 × 0.15 × 1.5	0.011
14	W14 × 211	W14 × 500	W21 × 182	0.075 × 0.15 × 1.5	0.010
15	W14 × 176	W14 × 500	W21 × 166	0.070 × 0.15 × 1.5	0.010
16	W14 × 132	W14 × 455	W14 × 211	0.065 × 0.15 × 1.5	0.012
17	W14 × 132	W14 × 455	W14 × 193	0.065 × 0.15 × 1.5	0.011
18	W14 × 132	W14 × 455	W14 × 159	0.065 × 0.15 × 1.5	0.010
19	W14 × 132	W14 × 455	W14 × 145	0.065 × 0.15 × 1.5	0.008
20	W14 × 132	W14 × 455	W14 × 120	0.065 × 0.15 × 1.5	0.005

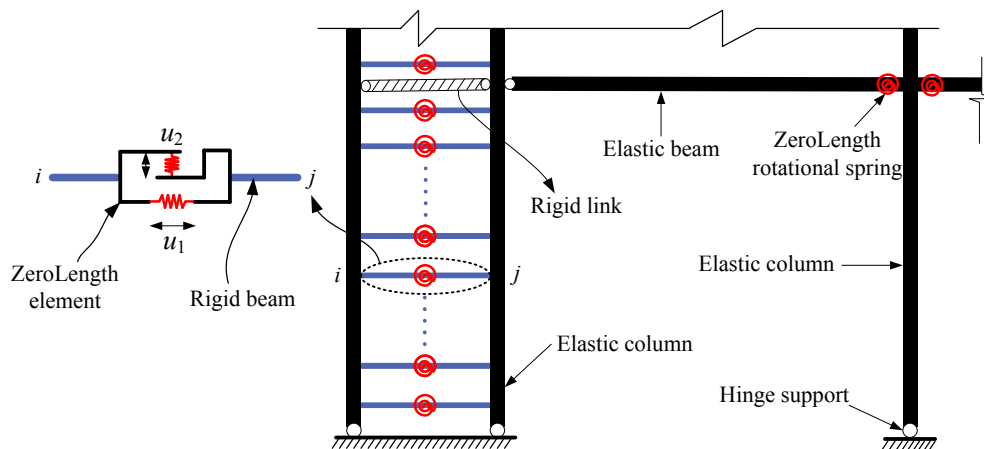


Fig. 16. Numerical modeling based on OpenSees.

(MCs) and non-yielding members (beam and column) adopt steel material with yielding stress of 345 MPa. The performance objectives, IO, RR and CP, corresponding to the three seismic hazard levels described in Section 3.4.1 are considered in the design process. The target RDR θ_y and θ_d for SLE and DBE level are selected as 0.17% and 0.58%, respectively. All the other design parameters can be calculated easily, and are listed in Table 1. The additional base shear resulted from P-Delta effect is not added as the stability coefficients are lower than 10%. By the proposed design flowchart in Fig. 5, the section of structural members are designed and listed in Table 2. The fundamental period of prototype building is 2.04 s, which is close to initial assumption 2.0 s. Hence, no iteration is performed for the prototype design.

5. Seismic performance assessment of the designed EDC-MF system

5.1. Numerical model

To assess the seismic performance of the designed EDC-MF system, a detailed nonlinear numerical model is built using OpenSees program [41]. Fig. 16 describes the numerical modeling approach. Because the beams and columns are capacity designed to remain elastic, they are modeled using elastic beam-column elements, and their maximum forces are checked in the post-processing. The links at story level of EDCs are simulated using rigid Link. The flexural behavior of MCs is modeled by zero-length elements and Steel4 material which is a general

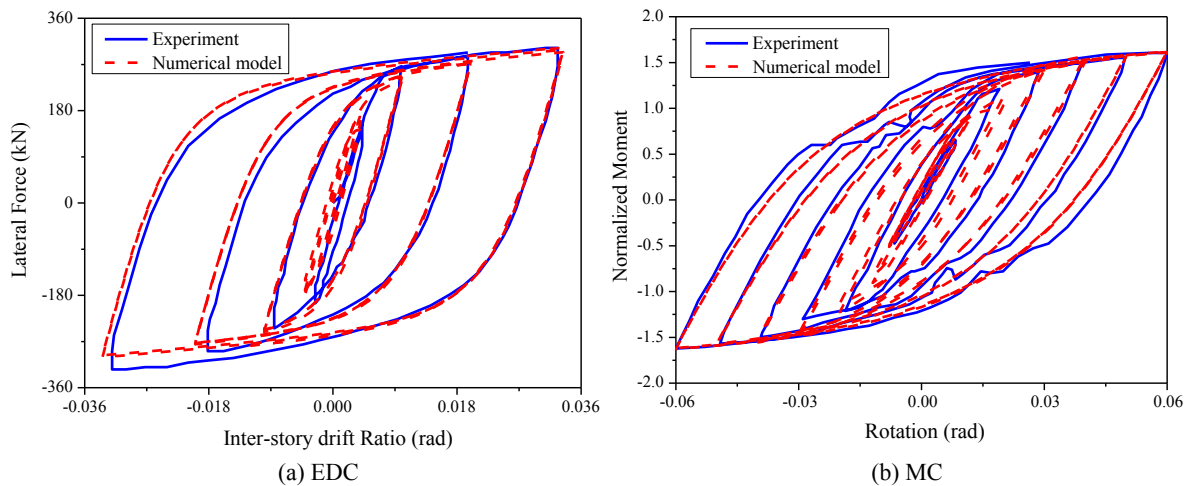


Fig. 17. Numerical model validation for the EDC and MC system.

uniaxial material with combined kinematic and isotropic hardening. The RSSDs in EDC are modeled utilizing a combination of zero-length element and rigid beams. The axial behavior u_1 of the zero-length element is simulated by elastic uniaxial material with elastic modulus same with the axial stiffness of RSSDs. And the shear behavior u_2 of the zero-length element is simulated by Steel4 material. The model parameters for Steel4 material are listed in Table A2. Fig. 17(a) and (b) gives the numerical and experimental result comparison of EDC and MC system, respectively. The experimental results originate from the quasi-static test conducted by Li [55] and Pryor [57]. The results show that the numerical model is able to predict the nonlinear behavior of RSSD and MC fuses. In addition, 2.5% Rayleigh damping are assigned to the numerical model for dynamic analysis.

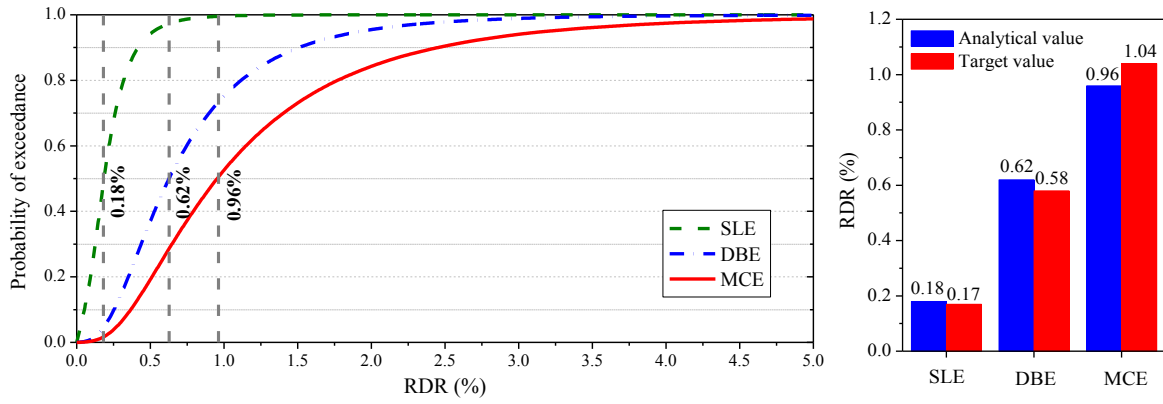
5.2. Results of nonlinear dynamic analyses

A suite of 20 ground motions, shown in Table A1, are respectively scaled to SLE, DBE and MCE level for nonlinear time history analysis of the designed 20-story EDC-MF system. Fig. 18 presents the results of the RDR and base shear probability of exceedance at the three seismic levels. These probability curves are constructed according to the maximum RDR and base shear responses of each earthquake record and the assumption of lognormal distribution. From this figure, the RDRs are 0.18%, 0.62% and 0.96% for SLE, DBE and MCE level, respectively, at the 50% probability of exceedance, which match well with the target RDRs, 0.17%, 0.58% and 1.04%, adopted during the design process. The base shear coefficient is defined as the ratio of the maximum base shear to the structural weight W . Thus, the base shear for SLE, DBE and MCE level are $0.084W$, $0.218W$ and $0.301W$, respectively, at the 50% probability of exceedance. Under SLE shaking level, the analytical value is identical to the design value $0.084W$. Under DBE and MCE shaking level, the analytical values are larger than the design values $0.166W$ and $0.211W$. The value of $0.211W$ is calculated according to V_y , V_p , the target roof drift ratio and post-yielding stiffness. Results reveal that the capacity of the designed structure is larger than the design seismic demand, and the designed structure is conservative.

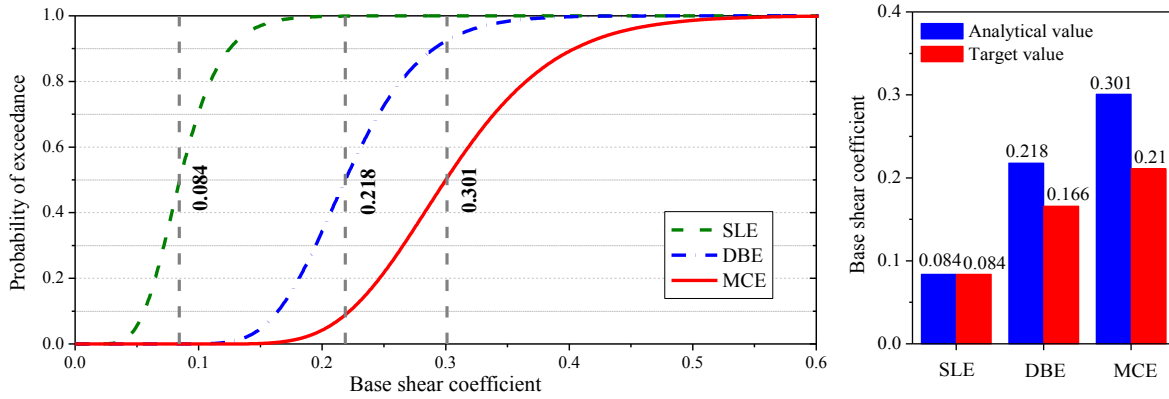
The maximum inter-story drift ratios of the designed structure subjected to different shaking intensities are shown in Fig. 19. In general, the inter-story drift ratios are lower at the top of the structure and are larger at the bottom, because the seismic demand of the yielding members are larger at the bottom floors and lower at the top floors (see

Figs. 20 and 21). The inter-story drift ratios of near-fault ground motions (NO. 11–20) are larger than far-field ground motions (NO. 1–10) on the whole, especially when subjected to ground motion NO. 15 and NO. 16, indicating that near-fault has significant influence on the structural dynamic responses due to its impulse effect. Following seismic design provisions in ASCE 7-10 [11], the EDC-MF system is designed to satisfy two design criteria [18,58]. The maximum inter-story drift ratio at the DBE and MCE hazard level are limited to 2.5% and 3.5%, respectively. Observed from Fig. 19, the maximum of mean inter-story drift ratio are 1.1% and 2.0% for DBE and MCE level, respectively, which indicates that mean value of the inter-story drift ratio at DBE and MCE hazard level are much less than the limitations. Moreover, considering the structural and non-structural damages, the SEAOC [34,59] defined three performance targets, 0.5%, 1.5% and 2.5%, corresponding to SLE, DBE and MCE hazard level, respectively. It can be found that the mean values of the inter-story drift ratio at the three seismic intensities are obviously less than the limitations of SEAOC. The maximum of mean inter-story drift ratio for SLE level is 0.26%. The above analysis results demonstrate that the designed EDC-MF system has good seismic performance against strong ground motions, and the proposed designed method is reliable for designing fused high-rise structures.

To evaluate performance of the yielding members, the shear demand capacity ratio (DCR) defined as the maximum shear to the yielding shear in RSSD fuses and the moment DCR defined as the maximum bending moment to the yielding moment in MC fuses are obtained via nonlinear time history results. Figs. 20 and 21 plot the shear and moment DCRs of each story at the three seismic hazard levels, respectively. For SLE hazard level, most of the shear DCRs and all of the moment DCRs are lower than 1. It means that most of the RSSDs remain elastic and no MC member enter inelastic phase. Few RSSDs enter inelastic phase only when subject to near-fault ground motion NO. 13, NO. 15 and NO. 16. The maximum values of mean shear and moment DCRs are 0.78 and 0.28, respectively. Therefore, the performance objective IO, which requires all the structural members to be elastic, is deemed to be achieved. For DBE hazard level, most shear DCRs are larger than 1, and most moment DCRs are lower than 1. The maximum values of mean shear and moment DCR are 1.57 and 0.93, respectively. It means that the RSSDs have yielded to dissipate seismic energy, while the MCs behave elastically. Due to the RSSD fuses can be easily replaced after an earthquake, the designed EDC-MF system is capable of achieving the performance objective RR. For MCE hazard level, almost all the shear DCRs are larger than

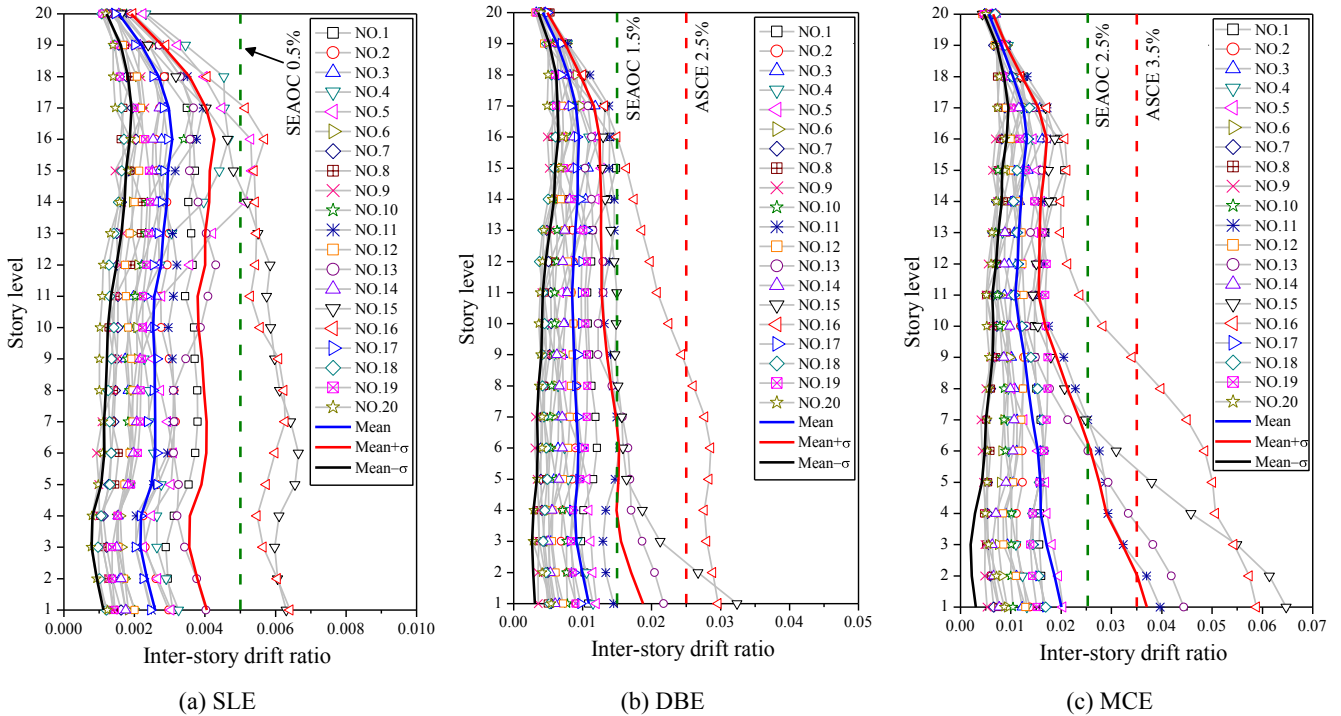


(a) RDR probability of exceedance and comparison with target values



(b) Base shear probability of exceedance and comparison with target values

Fig. 18. Probability of exceedance for RDR and base shear of the designed EDC-MF.



(a) SLE

(b) DBE

(c) MCE

Fig. 19. The maximum inter-story drift ratio of the designed EDC-MF.

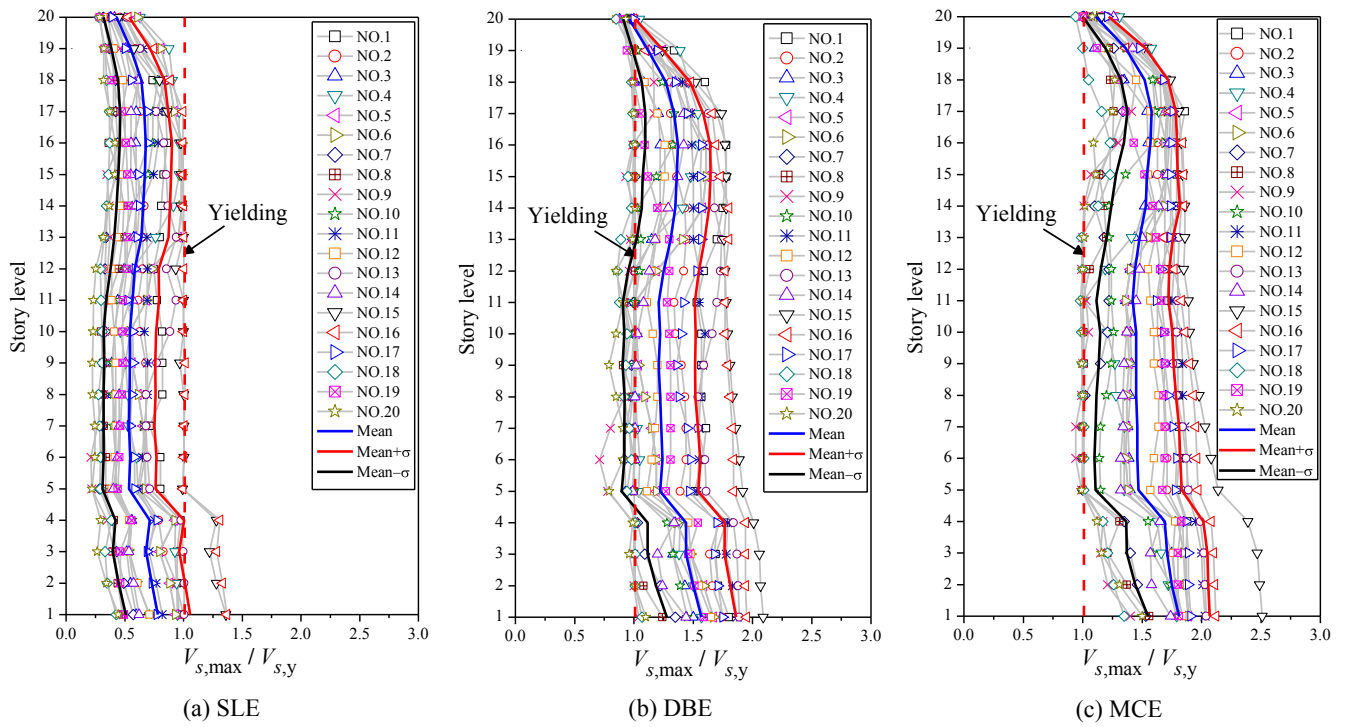


Fig. 20. The shear DCR of RSSDs.

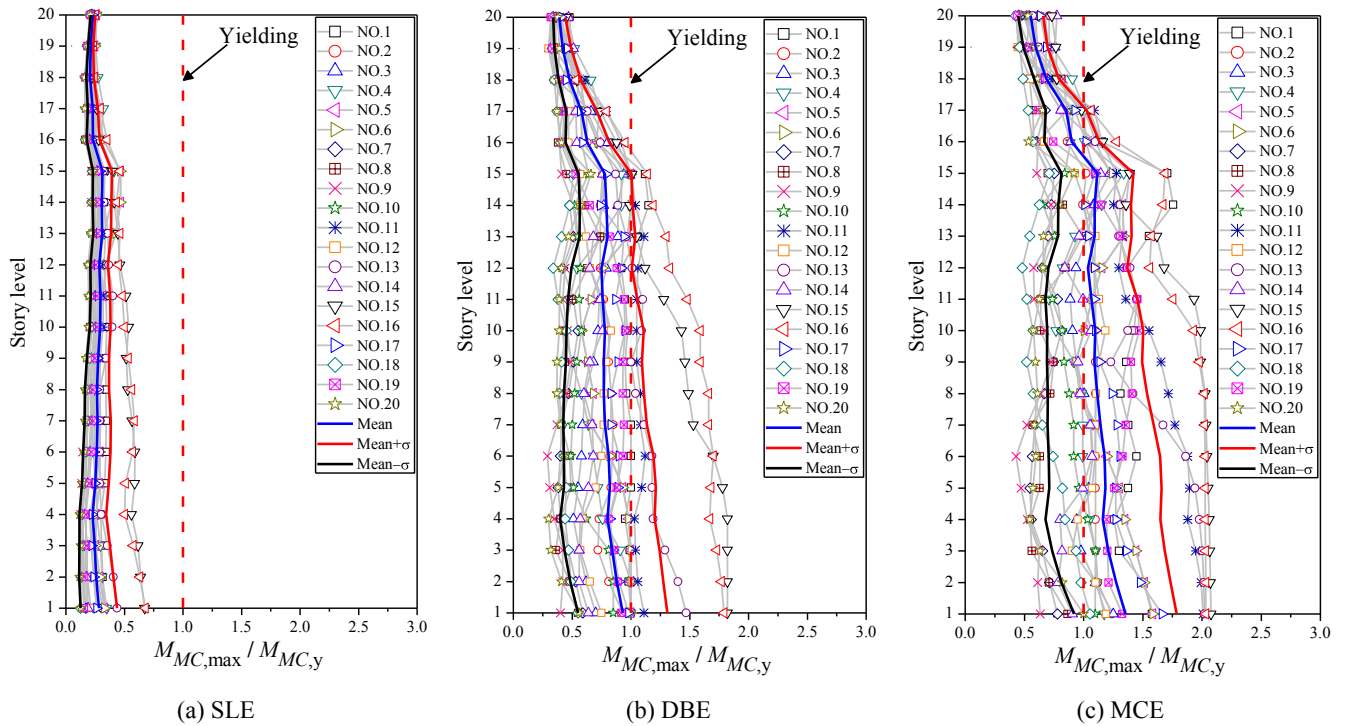
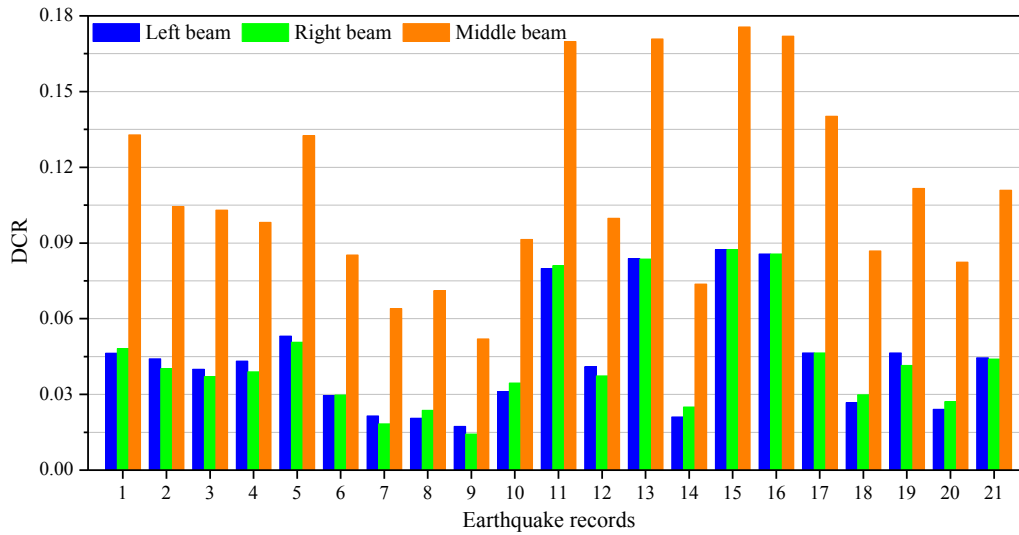
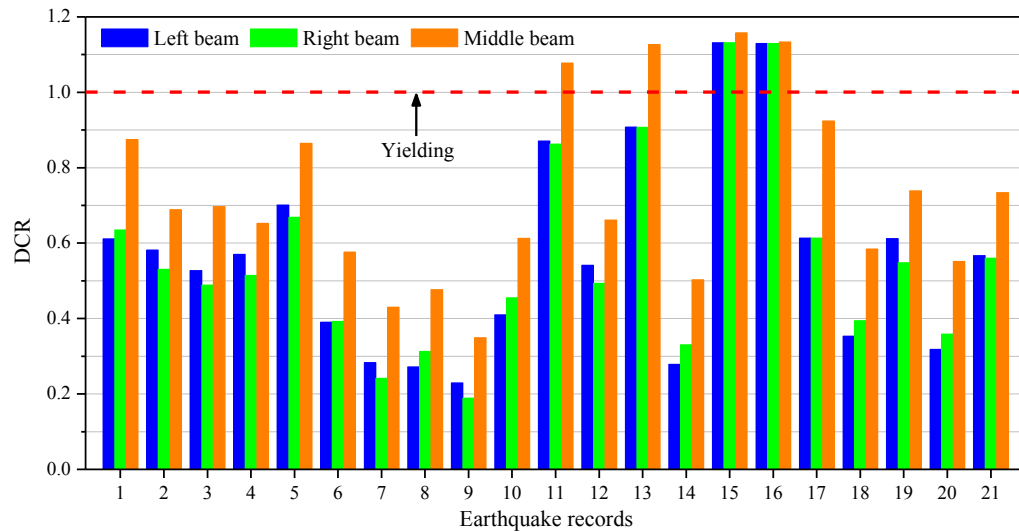


Fig. 21. The moment DCR of MCs.



(a) Shear DCR



(b) Moment DCR

Fig. 22. The shear and moment DCR of the first story beams at MCE hazard level.

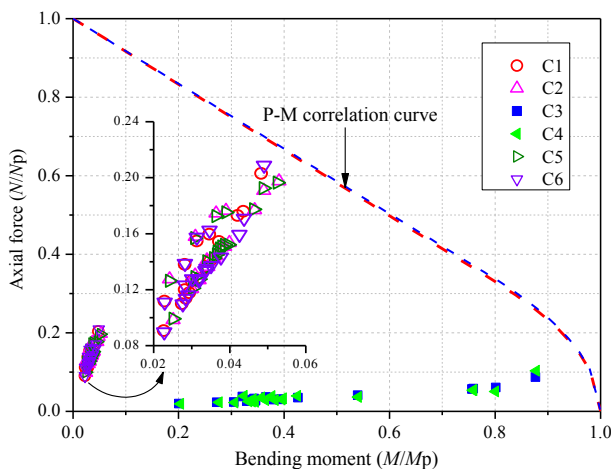


Fig. 23. P-M interactions of the column bases at MCE hazard level.

1, and most moment DCRs are larger than 1. The maximum values of mean shear and moment DCR are 1.81 and 1.35, respectively. Both the RSSD and MC fuses have yielded to protect the gravity system from damage, which allows the designed EDC-MF system to target performance objective CP. The yielding mechanism of the EDC-MF follows the sequence of RSSDs yield at DBE level and MCs yield at MCE level, which is in accordance with the pre-selected yielding mechanism. The results reveal that the proposed design method is able to achieve the prescribed yielding mechanism and performance objectives.

In order to check the performance of non-yielding members in gravity-resisting system, the shear and moment DCRs of the beams under the excitation of MCEs are obtained from the nonlinear dynamic analyses. Because the seismic demand of yielding members and inter-story drift ratio are largest at the first story, only the first story beams where plastic hinges are most likely to occur, are discussed here. Fig. 22 depicts the shear and moment DCRs of the first story beams, and the earthquake record NO. 21 represents the mean value of NO. 1–20. Because the left and right beams are hinged to the EDCs and the middle beam are assembled with more MC, the

shear and moment DCRs of middle beam are larger than left and right beams. The maximum value of shear DCRs is 0.176, which is much lower than 1. There are four near-fault earthquake records in which the moment DCRs are larger than 1. The maximum value of moment DCR is 1.158. Although the beams enter inelastic phase under the excitation of these four records, the nonlinear behavior is slight. And mean values of the moment DCR for left, right and middle beam are obviously less than 1, which are 0.567, 0.560 and 0.734, respectively. Hence, the proposed designed method is deemed to be capable of protecting the beam members from yielding. Moreover, it can be observed that the shear DCRs are much less than the moment DCRs, indicating the function of strong shear-weak bending design concept.

According to the maximum internal force responses, Fig. 23 provides the P-M interactions of the column bases at MCE hazard level, where the C1–C6 represent the six column bases in Fig. 15 from left to right, and the vertical and horizontal axes represent the nominalized axial force and bending moment. The blue dash line represents P-M curve of column C3 and C4, while red dash line represents P-M curve of other columns. N and M are the maximum axial force and moment of columns, respectively. N_p is the production of section area and yielding strength, and M_p is the production of section modulus and yielding strength. For the columns in the EDC (C1, C2, C5, C6), the nominal axial force is larger than the nominal moment because these columns are dominated by axial load. Since the frame columns (C3, C4) are dominated by bending moment, their nominal moment is larger than the nominal axial force. In this figure, all points are distributed below the limit curve, illustrating that no plastic hinge appears under excitation of MCEs, and the columns behave elastically. A few beams have entered yielding phase under seismic excitations (Fig. 22), while all the columns remain elastic, indicating the function of strong column-weak beam design concept.

6. Discussion

The proposed design method is accurate and effective, and some further works may need to be conducted in the future. When the structural torsional effect resulted from the asymmetric plan is significant, the iteration number of the proposed design method may increase, and the design accuracy may decrease. Asymmetric geometries in elevation by non uniform stiffness can also influence the design accuracy of our method. To improve these aspects fully, some effects should be taken into account: (a) the seismic torsional moment should be considered for torsional design of structural components; (b) more structure periods may need to be estimated for the design; (c) the energy modification factors should be modified to consider the significant torsional effect. The 2DMPA method introduced by Birzhandi [60] and Lin [61] can be utilized for improving it. The soil-structure interactions and seismic cumulative damage have an obvious effect on the dynamic characteristics and hysteretic behavior of the structure. To fully consider these effects, the story model for calculating energy modification factors should be modified. Soil-structure interactions should be simulated in the story model, an effective way is to use spring element to model the interactions [62]. And a hysteretic model considering cumulative damage should be adopted in the nonlinear dynamic analysis. The method presented in this paper is for the design of horizontal seismic excitation. For vertical earthquake, the method presented in this paper is also applicable. Several parameters need to be modified: (a) the vertical mode should be considered, and the energy modification factors need to be modified by the vertical seismic excitation; (b) the structural members need to be designed under vertical seismic action. When considering the action of horizontal and vertical earthquake simultaneously, a combination of multi-directional seismic excitation designed in the code [13] can be used. Although the performance objective CP can be ensured by the proposed design method, the progressive collapse of the designed structure may still occur under extreme earthquakes. The effects of progressive collapse failure modes need

to be discussed in the future.

7. Conclusions

This study presents an improved PBPD method, which simultaneously considers the design of multiple performance objectives, the post-yield stiffness and high-mode effect. The derivation of the improved method has been illustrated in detail. And a novel dual structure, 20-story EDC-MF, is designed and numerically modeled to demonstrate the effectiveness of the proposed method. During the design process and nonlinear dynamic analysis, the following conclusions are drawn:

- (1) The proposed design procedure is simple and can simultaneously and effectively achieve the design of multiple performance objectives for SLE, DBE and MCE hazard level. And its effectiveness for designing seismic resilient fused high-rise building has been proved.
- (2) The 20-story EDC-MF designed by the proposed method achieves the target roof drift ratios and fundamental period without iteration. The base shear of dynamic analysis is identical to the design value at SLE shaking level, and is conservative at DBE and MCE shaking level.
- (3) The pre-selected yielding mechanism can be achieved by the proposed method. In the designed EDC-MF system, all structural members remain elastic at SLE hazard level. During DBE hazard level, the primary fuses, RSSDs, enter inelastic phase while the secondary fuses, MCs, behave elastically. For MCE hazard level, both RSSDs and MCs yield to protect gravity-resisting members from damage.
- (4) The inter-story drift ratio of the designed EDC-MF system is less than the limitation in the code, indicating that the designed EDC-MF system has good seismic performance against strong ground motions. The novel EDC-MF system can be applied to high-rise building as a seismic resilient fused structure.

Data availability

The data used to support the findings of this study are included within the article.

Disclosure

Any opinions, findings, and conclusions or recommendations expressed in this paper are those of the authors.

Declaration of Competing Interest

The authors declare that they have no conflicts of interest.

Acknowledgements

The authors are grateful for the financial support from the Fundamental Research Funds for the Central Universities of Central South University (Project No. 502221804), the National Natural Science Foundation of China (Project No. 51878674), the Foundation for Key Youth Scholars in Hunan Province and the Project of Yuying Plan in Central South University. Any opinions, findings, and conclusions or recommendations expressed in this paper are those of the authors.

Appendix A

See Figs. A1–A3, Tables A1 and A2.

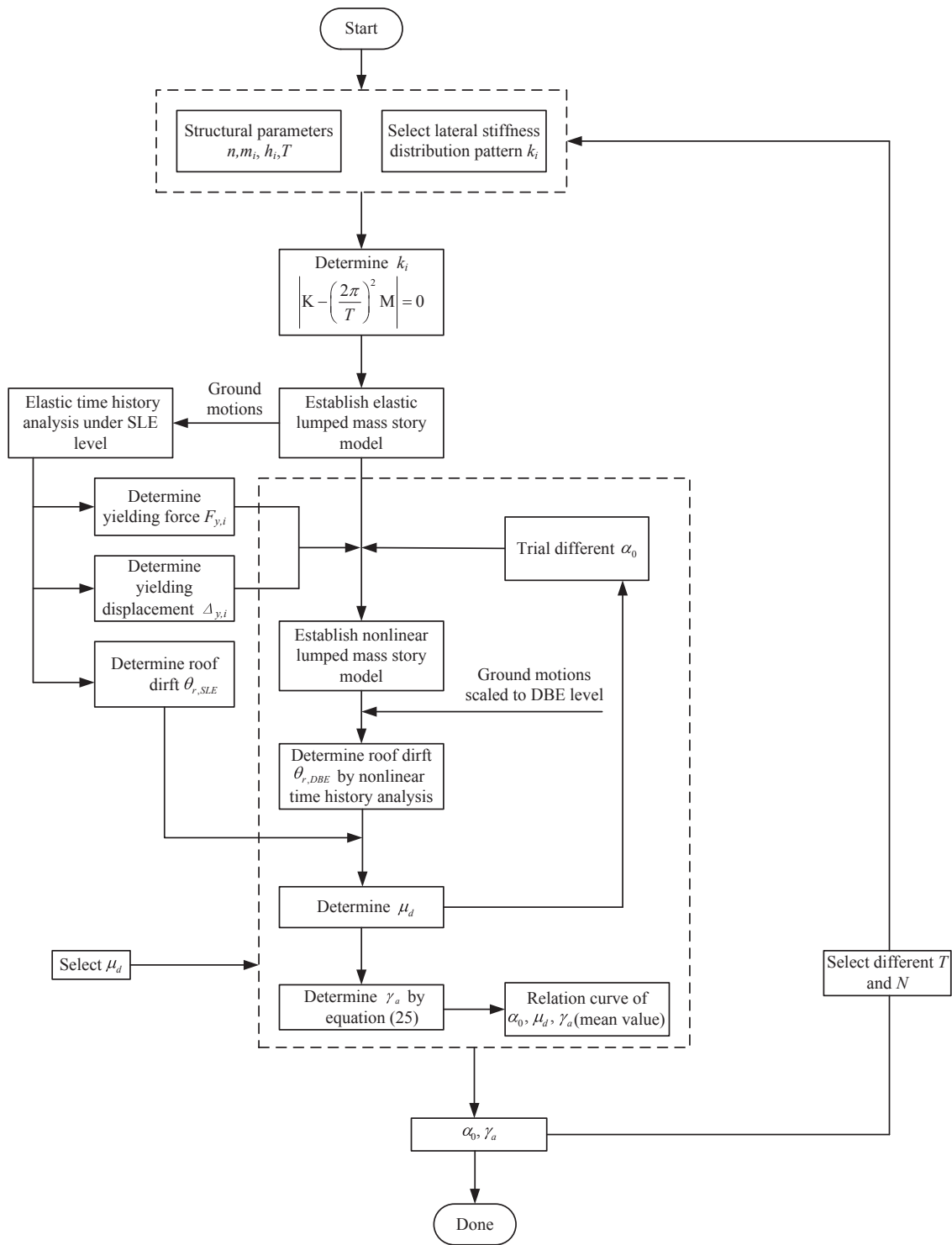


Fig. A1. Flowchart for determining γ_a .

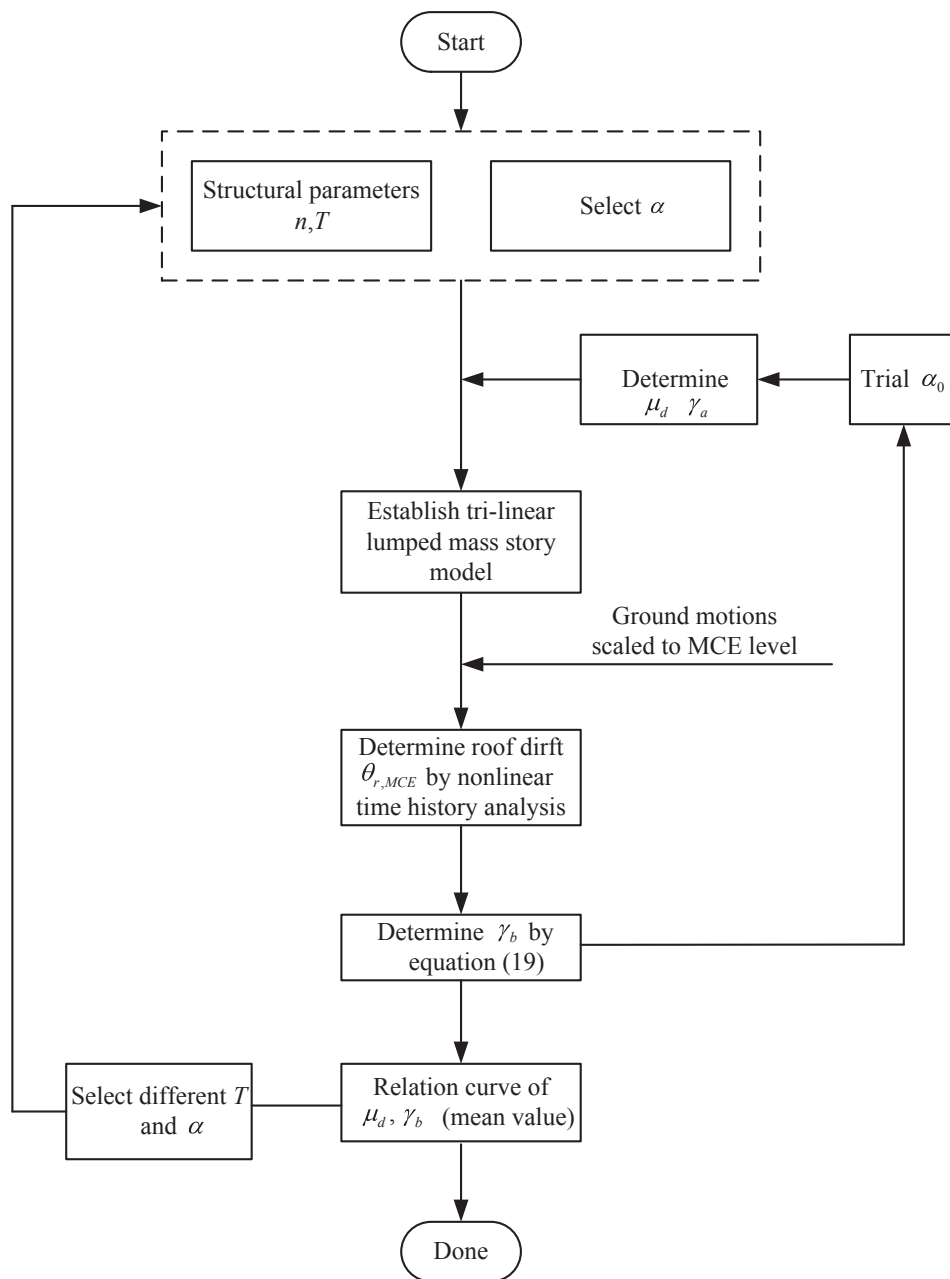


Fig. A2. Flowchart for determining γ_b .

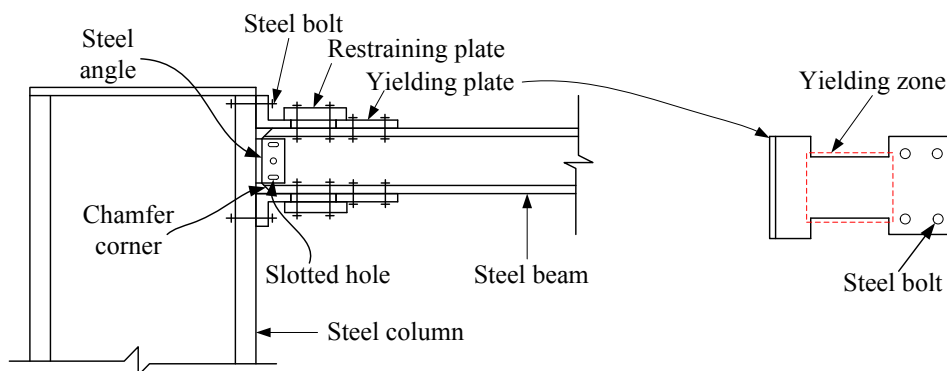


Fig. A3. Beam-to-column connection.

Table A1
Earthquake records for nonlinear time history analysis.

No.	Earthquake	Year	Magnitude	NGA#	Station	Fault distance (km)	Epicenter depth (km)
1	Kern County	1952	7.36	14	SBC	82.19	16
2	Loma Prieta	1989	6.93	742	BV-F	61.71	16.5
3	Loma Prieta	1989	6.93	749	B-SC	78.41	16.5
4	Loma Prieta	1989	6.93	794	SF-DH	71.33	16.5
5	Loma Prieta	1989	6.93	796	SFP	77.43	16.5
6	Loma Prieta	1989	6.93	798	SF-TH	76.5	16.5
7	Northridge-01	1994	6.69	1037	M-OCC	75.8	17.5
8	Northridge-01	1994	6.69	1060	RC-DC	79.99	17.5
9	Northridge-01	1994	6.69	1073	SP-PV	57.03	17.5
10	Northridge-01	1994	6.69	1093	VP-SA	77.56	17.5
11	Chi-Chi_Taiwan	1999	7.62	1193	CHY024	9.62	8
12	Chi-Chi_Taiwan	1999	7.62	1489	TCU049	3.76	8
13	Chi-Chi_Taiwan	1999	7.62	1494	TCU054	5.28	8
14	Chi-Chi_Taiwan	1999	7.62	1512	TCU078	8.2	8
15	Chi-Chi_Taiwan	1999	7.62	1530	TCU103	6.08	8
16	Chi-Chi_Taiwan	1999	7.62	1545	TCU120	7.4	8
17	Chi-Chi_Taiwan	1999	7.62	1546	TCU122	9.34	8
18	Chi-Chi_Taiwan	1999	7.62	1549	TCU129	1.83	8
19	Duzce_Turkey	1999	7.14	1611	Lamont 1058	0.21	13
20	Duzce_Turkey	1999	7.14	1612	Lamont 1059	4.17	13

Table A2
Model parameters for steel4 material.

Fuse	b_k	R_0	r_1	r_2	b_l	b_l	ρ_l	R_l	I_{yp}
RSSD	0.01	20	0.9	0.15	0.2	0.84	0.0006	3.0	1.0
MC	0.01	15	0.9	0.15	0.2	0.84	0.0006	3.0	1.0

Note: the definition of each item can refer to Ref. [41].

References

- Wang J, Zhao H. High performance damage-resistant seismic resistant structural systems for sustainable and resilient city: a review. *Shock Vib* 2018;2018:1–32.
- Yang TY, Atkinson JC, Tobber L. Detailed seismic performance assessment of high-value-contents laboratory facility. *Earthq Spectra* 2014;31(4): 141208072728004.
- Guo W, Zhai Z, Cui Y, et al. Seismic performance assessment of low-rise precast wall panel structure with bolt connections. *Eng Struct* 2019;181:562–78.
- Guo W, Zhai Z, Yu Z, et al. Facility performance indexes and rapid test feasibility evaluation method of shaking tables. *KSCE J Civ Eng* 2019;23(7):3097–112.
- Guo W, Zhai Z, Yu Z, et al. Experimental and numerical analysis of the bolt connections in a low-rise precast wall panel structure system. *Adv Civ Eng* 2019. Article ID 7594132, 23 pages.
- Guo W, Zhai Z, Wang H, et al. Shaking table test and numerical analysis of an asymmetrical twin-tower super high-rise building connected with long-span steel truss. *Struct Design Tall Spec Build* 2019:e1630.
- Cimellaro GP. New trends on resiliency research. 16th world conference on earthquake engineering, 2017. 16WCEE, Chile. 2017.
- Mahin Stephen. Resilience by design: a structural engineering perspective. 16th world conference on earthquake engineering, 2017. 16WCEE, Chile. 2017.
- ASCE/SEI Sustainability Committee; 2014 [<http://www.asce.org/sustainability/>].
- Grigorian M, Moghadam AS, Mohammadi H, Kamizi M. Methodology for developing earthquake-resilient structures. *Struct Design Tall Spec Build* 2018:e1571.
- ASCE 7-10. Minimum design loads for buildings and other structures. American Society of Civil Engineers (ASCE); 2010.
- National Building Code of Canada (NBCC). Division B Part 4 structural design. Ottawa: NBCC; 2005.
- GB 50011-2010. Code for seismic design of buildings. Beijing: China Architecture & Building Press; 2010.
- Yang TY, Tung DP, Li Y. Equivalent energy design procedure for earthquake resilient fused structures. *Earthq Spectra* 2018;34(2):795–815.
- Vargas R, Bruneau M. Analytical response and design of buildings with metallic structural fuses. I. *J Struct Eng* 2009;135(4):386–93.
- Roeder C, Popov E. Inelastic behavior of eccentrically braced steel frames under cyclic loadings. NASA STI/Recon Tech Rep N 1977;78:20375.
- Aristizabal-Ochoa Datio J. Disposable knee bracing: improvement in seismic design of steel frames. *J Struct Eng* 1986;112(7):1544–52.
- Li T, Yang TY, Tong G. Performance-based plastic design and collapse assessment of diagrid structure fused with shear link. *Struct Design Tall Spec Build* 2019:e1589.
- Dorian PT. Design and validation of innovative earthquake resilient fused structures (PhD thesis). Vancouver: The University of British Columbia; 2017.
- Etebarian Hamidreza. Seismic design and performance evaluation of dual-fused H-frame system (Master degree Thesis) Vancouver: The University of British Columbia; 2018.
- Vargas R, Bruneau M. Experimental response of buildings designed with metallic structural fuses. II. *J Struct Eng* 2009;135(4):394–403.
- Lu X, Zhang L, Cui Y, et al. Experimental and theoretical study on a novel dual-functional replaceable stiffening angle steel component. *Soil Dyn Earthq Eng* 2018;114:378–91.
- Li G, Pang M, Sun F, et al. Seismic behavior of coupled shear wall structures with various concrete and steel coupling beams. *Struct Design Tall Spec Build* 2018;27:e1405.
- Guo W, Wu J, Hu Y, et al. Seismic performance evaluation of typical dampers designed by Chinese building code. *Earthq Eng Eng Vib* 2019;18(2):433–46.
- Yu Z, Liu H, Guo W, et al. A general spectral difference method for calculating the minimum safety distance to avoid the pounding of adjacent structures during earthquakes. *Eng Struct* 2017;150:646–55.
- Guo W, Wu X, Wei X, et al. Inductance effect of passive electromagnetic dampers on building-damper system subjected to near-fault earthquakes. *Adv Struct Eng* 2019:1–20. <https://doi.org/10.1177/1369433219870579>.
- Guo W, Hu Y, Li Y, Zhai Z. Seismic performance evaluation of typical dampers designed by Chinese Code subjected to the main shock-aftershocks. *Soil Dyn Earthq Eng* 2019;126:1–13. <https://doi.org/10.1016/j.soildyn.2019.105829>.
- Shoebi S, Kafi MA, Gholhaki M. New performance-based seismic design method for structures with structural fuse system. *Eng Struct* 2017;132:745–60.
- Bedon C, Amadio C. Numerical assessment of vibration control systems for multi-hazard design and mitigation of glass curtain walls. *J Build Eng* 2018;15:1–13.
- Medhekar MS, Kennedy DJL. Displacement-based seismic design of buildings-theory. *Eng Struct* 2000;22(3):201–9.
- Yang B, Lu X. Displacement-based seismic design approach for prestressed precast concrete shear walls and its application. *J Earthq Eng* 2017:1–25.
- Panagiotou M, Restrepo José I. Displacement-based method of analysis for regular reinforced-concrete wall buildings: application to a full-scale 7-story building slabe tested at UC-San Diego. *J Struct Eng* 2011;137(6):677–90.
- Chao SH, Goel SC. Performance-based plastic design of seismic resistant special truss moment frames. *AISC Eng J Second Quarter* 2008:127–50.
- Goel SC, Liao WC, Bayat MR, et al. Performance-based plastic design (PBSD) method for earthquake-resistant structures: an overview. *Struct Design Tall Spec Build* 2010;19(1–2):115–37.
- Qiu CX, Zhu S. Performance-based seismic design of self-centering steel frames with SMA-based braces. *Eng Struct* 2017;130:67–82.
- Bai J, Ou J. Earthquake-resistant design of buckling-restrained braced RC moment frames using performance-based plastic design method. *Eng Struct* 2016;107:66–79.
- Li T, Yang TY, Tong S, et al. Performance-based seismic design and evaluation of fused steel diagrid frame. *Earthq Spectra* 2018;34(4):1869–91.
- Qiang H, Feng P, Qu Z. Seismic responses of post yield hardening single-degree-of-freedom systems incorporating high-strength elastic material. *Earthq Engng Struct Dyn* 2019:1–23.
- Liao K, Wang Y, Chen C. Probabilistic seismic performance evaluation of steel moment frame using high-strength and high-ductility steel. *Constr Build Mater* 2018;184:151–64.
- Li Y, Li G, Jiang J, et al. Mitigating seismic response of RC moment resisting frames using steel energy-dissipative columns. *Eng Struct* 2018;174:586–600.
- Mazzoni S, McKenna F, Scott MH, Fenves GL. Open system for engineering simulation user-command-language manual, version 2.0 Pacific Earthquake Engineering Research Center Berkeley (CA): Univ California; 2009.
- Newmark NM, Hall WJ. Earthquake spectra and design. Berkeley: Earthquake Engineering Research Institute; 1982.
- Bai J, Yang TY, Ou J. Improved performance-based plastic design for RC moment resisting frames: development and a comparative case study. *Int J Struct Stab Dyn*

- 2018;18(4):1850050.
- [44] Housner GW. Limit design of structures to resist earthquakes. Proceedings of the world conference on earthquake engineering, 5. 1956. p. 1–11.
- [45] Akiyama H. Earthquake-resistant limit-state design of buildings. Japan: University of Tokyo Press; 1985.
- [46] IBC: International Building Code. International Code Council; 2006.
- [47] NRCC: National Building Code of Canada. Associate Committee on the National Building Code. National Research Council of Canada; 2010.
- [48] Chao SH, Goel SC, Lee SS. A seismic design lateral force distribution based on inelastic state of structures. *Earthq Spectra* 2007;23(3):547–69.
- [49] AISC 341-10. Seismic provisions for structural steel buildings (ANSI/AISC341-10); 2010.
- [50] Pacific Earthquake Engineering Research Center (PEER). PEER ground motion database; 2011. Available at http://peer.berkeley.edu/products/strong_ground_motion_db.html.
- [51] Yang TY, Moehle JP, Bozorgnia Y, et al. Performance assessment of tall concrete core-wall building designed using two alternative approaches. *Earthq Eng Struct Dyn* 2012;41(11):1515–31.
- [52] Miranda E. Approximate seismic lateral deformation demands in multistory buildings. *J Struct Eng* 1999;125(4):417–25.
- [53] Xiong C, Lu X, Guan H, et al. A nonlinear computational model for regional seismic simulation of tall buildings. *Bull Earthq Eng* 2016;14(4):1047–69.
- [54] Miranda E, Reyes CJ. Approximate lateral drift demands in multistory buildings with nonuniform stiffness. *J Struct Eng* 2002;128(7):840–9.
- [55] Li YW, Li GQ, Sun FF, et al. Experimental study on continuous energy-dissipative steel columns under cyclic loading. *J Constr Steel Res* 2018;141:104–17.
- [56] Li YW, Li GQ, Jiang J, et al. Modeling of behavior of continuous energy-dissipative steel columns under cyclic loads. *J Earthq Eng* 2017:1–24.
- [57] Pryor SE, Murray TM. Next generation partial strength steel moment frame connections for seismic resistance. *Res Dev Pract Struct Eng Constr* 2012. St-145-0423.
- [58] Yang TY, Li Y, Goel SC. Seismic performance evaluation of long-span conventional moment frames and buckling-restrained knee-braced truss moment frames. *J Struct Eng* 2015. 04015081.
- [59] SEAOC. Performance based seismic engineering of buildings. Vision 2000 report vols. I and II. Sacramento (California): Structural Engineers Association of California; 1995.
- [60] Birzhandi MS, Halabian AM. Application of 2DMPA method in developing fragility curves of plan-asymmetric structures. *Eng Struct* 2017;153:540–9.
- [61] Lin J, Tsai K. Simplified seismic analysis of asymmetric building systems. *Earthq Eng Struct Dyn* 2007;36(4):459–79.
- [62] Xiong W, Jiang LZ, Li YZ. Influence of soil–structure interaction (structure-to-soil relative stiffness and mass ratio) on the fundamental period of buildings: experimental observation and analytical verification. *Bull Earthq Eng* 2016;14(1):139–60.